Plant, Cell & Environment

Plant, Cell and Environment (2015) **38**, 2353–2371 doi: 10.1111/pce.12555

Original Article

Tobacco guard cells fix CO_2 by both Rubisco and PEPcase while sucrose acts as a substrate during light-induced stomatal opening

Danilo M. Daloso[1,2], Werner C. Antunes[1,3], Daniela P. Pinheiro[1], Jardel P. Waquim[1], Wagner L. Araújo[1], Marcelo E. Loureiro[1], Alisdair R. Fernie[2] & Thomas C. R. Williams[1,4]

[1]Departamento de Biologia Vegetal, Universidade Federal de Viçosa, Viçosa 36570-900 Minas Gerais, Brazil, [2]Max-Planck-Institut für Molekulare Pflanzenphysiologie, Potsdam-Golm 14476, Germany, [3]Departamento de Biologia, Universidade Estadual de Maringá, Maringá, Paraná 87020-900, Brazil and [4]Departamento de Botânica, Universidade de Brasilia, Brasilia, Distrito Federal 70910-900, Brazil

ABSTRACT

Transcriptomic and proteomic studies have improved our knowledge of guard cell function; however, metabolic changes in guard cells remain relatively poorly understood. Here we analysed metabolic changes in guard cell-enriched epidermal fragments from tobacco during light-induced stomatal opening. Increases in sucrose, glucose and fructose were observed during light-induced stomatal opening in the presence of sucrose in the medium while no changes in starch were observed, suggesting that the elevated fructose and glucose levels were a consequence of sucrose rather than starch breakdown. Conversely, reduction in sucrose was observed during light- plus potassium-induced stomatal opening. Concomitant with the decrease in sucrose, we observed an increase in the level as well as in the ^{13}C enrichment in metabolites of, or associated with, the tricarboxylic acid cycle following incubation of the guard cell-enriched preparations in ^{13}C-labelled bicarbonate. Collectively, the results obtained support the hypothesis that sucrose is catabolized within guard cells in order to provide carbon skeletons for organic acid production. Furthermore, they provide a qualitative demonstration that CO_2 fixation occurs both via ribulose-1,5-biphosphate carboxylase/oxygenase (Rubisco) and phosphoenolpyruvate carboxylase (PEPcase). The combined data are discussed with respect to current models of guard cell metabolism and function.

Key-words: guard cell metabolism; organic acids; Stable isotope labelling.

INTRODUCTION

Guard cells are specialized leaf epidermal cells that surround the stomatal pore. Changes in guard cell turgor determine the opening or closure of the stomatal pore which in turn regulates CO_2 uptake and water loss by transpiration. Although changes in guard cell metabolism during abscisic acid-induced stomatal closure have been studied in depth (Jin *et al*. 2013), there remain gaps in our knowledge regarding guard cell metabolism during stomatal opening. Given that stomatal aperture regulates gas exchange through the leaf epidermis and therefore determines water-use efficiency at the whole plant level (Lawson & Blatt 2014), a better understanding of guard cell function within processes regulating stomatal aperture is of fundamental importance for our understanding of the relationship between carbon assimilation and leaf transpiration in fluctuating environments (Hetherington & Woodward 2003). In this respect, the manipulation of guard cell metabolism has significant potential biotechnological application as it offers a route to greater water-use efficiency (Yang *et al*. 2005; Antunes *et al*. 2012; Lawson & Blatt 2014; Lawson *et al*. 2014; Medeiros *et al*. 2015).

Guard cell metabolism has been investigated for almost an entire century. Initial studies predicted that the interconversion of starch and sugars would be the mechanism regulating the dynamics of stomatal movements. It was therefore proposed that stomatal opening would depend on starch breakdown and an increase in sugar levels (Sayre 1923, 1926). However, this theory was superseded following the demonstration that cations can also act as osmolytes in guard cells (Fischer & Hsiao 1968; Humble & Hsiao 1970). The use of labelled ions (^{86}Rb, ^{42}K and ^{82}Br) and different salts (KCl, KNO_3, K_2SO_4 and KBr) helped to highlight the importance of ions for charge balance across the guard cell membrane and hence for stomatal movements (Humble & Hsiao 1970; Fischer 1971; MacRobbie 1981). These experiments were essential in demonstrating the importance of potassium (K^+) for guard cell osmoregulation (Vavasseur & Raghavendra 2005; MacRobbie 2006). The stomatal opening induced by K^+ salts is mediated by the blue light activation of H^+-ATPase pumps that results in membrane hyperpolarization that in turn enables the influx of K^+ by the opening of voltage-gated inward-rectifying K^+ channels (Shimazaki *et al*. 2007; Chen *et al*. 2012). It is now widely accepted that Cl^- and NO_3^- are the two main inorganic counter ions that balance the positive electrical charge of K^+ (Zeiger 1983; Guo *et al*. 2003; Kim *et al*. 2010). However,

Correspondence: T. C. R. Williams. e-mail: tcrwilliams@unb.br

these inorganic ions are unable to fully balance the positive electrical charge of K^+, leading to the synthesis and/or import of organic counter ions such as malate (Hedrich & Marten 1993; Outlaw 2003; Araújo *et al*. 2011a). The need to provide energy for ion uptake and carbon skeletons to act as counter ions therefore connects ion balance to metabolism in guard cells.

Despite receiving significant research attention, several questions remain concerning guard cell metabolism. For instance, the mode of CO_2 fixation and the distribution of photosynthetic fluxes are still controversial. Indeed although guard cells from C3 plants may present metabolism similar to cells with C_4 metabolism or crassulacean acid metabolism (CAM) (Outlaw & Kennedy 1978; Brown & Outlaw 1982; Outlaw 1989; Gautier *et al*. 1991; Vavasseur & Raghavendra 2005; Lawson & Blatt 2014; Lawson *et al*. 2014), the presence of C_3 metabolism in guard cells has also been reported (Gotow *et al*. 1988). Furthermore, the role of sucrose, suggested as merely being an osmolyte for guard cell regulation (Talbott & Zeiger 1998; Zeiger *et al*. 2002), has recently been revisited (Antunes *et al*. 2012; Kelly *et al*. 2013). Recent work suggests that sucrose plays a non-osmotic role in guard cell processes including inducing stomatal closure (Kelly *et al*. 2013). A recent publication from our group suggests that sucrose can act as a respiratory substrate in order to support stomatal function (Antunes *et al*. 2012); transgenic plants with higher capacity to cleave sucrose within their guard cells displayed greater stomatal conductance (Antunes *et al*. 2012). However, the fate of carbon released through sucrose degradation and its importance in stomatal movements remains to be elucidated. For this reason, it is imperative that changes in guard cell metabolism in the light or during stomatal movement are studied in greater detail.

Guard cells are highly responsive, exhibiting both a high capacity for ion and metabolite transport between them and their surrounding apoplastic space and a metabolism that is capable of dynamic change within a relatively short time period. For these reasons, the presence of a metabolic steady state is almost impossible to verify in these cells, complicating attempts to determine metabolic fluxes and model guard cell metabolism (Medeiros *et al*. 2015). Indeed, steady–state metabolic flux analysis cannot readily be applied to the analysis of fluxes in tissues that are undergoing marked diurnal variations in metabolic activities (Colón *et al*. 2009). However, dynamic labelling approaches, used to measure the time course of the labelling through the network, are highly particularly effective for autotrophic tissues and in situations in which only a short experimental period is desirable (Fernie *et al*. 2005; Ratcliffe & Shachar-Hill 2006). Considering the above-described defining features of guard cells, here we carried out several time course stomatal opening experiments in order to determine changes in guard cell metabolism during light-induced stomatal opening. We induced stomatal opening by incubating guard cell-enriched epidermal fragments in the light in the presence of K^+ or sucrose in the medium. Two hypotheses concerning the role of sucrose in the guard cell symplast during light-induced stomatal opening were tested here: (1) that sucrose is not degraded and acts solely as an osmolyte and (2) that sucrose is, at least partially, degraded to produce other metabolites. The first hypothesis is based on studies from Talbott & Zeiger (1998) who proposed that sucrose functions as an osmolyte molecule for guard cell osmoregulation. The second is based on data from previous study by our group suggesting that sucrose breakdown, and not just sucrose accumulation, is important during stomatal opening (Antunes *et al*. 2012). Furthermore, we carried out an isotope kinetic labelling experiment using ^{13}-$NaHCO_3^-$ in order to understand the distribution of photosynthetic fluxes in guard cells. The results of these experiments are discussed both in the context of the role of sucrose in general and with respect to current models of metabolic shifts associated with stomatal regulation.

MATERIALS AND METHODS

Plant material and growth conditions

Seeds of *Nicotiana tabacum* L. were surface decontaminated by shaking in 70% ethanol for 1 min and rinsing with sterile distilled H_2O. They were then treated with 2% sodium hypochlorite for 5 min and rinsed three times with sterile distilled H_2O. The seeds were then allowed to germinate in Petri dishes containing MS medium (Murashige & Skoog 1962) and were cultivated *in vitro* for 15 days. The seedlings were transplanted to 0.1 L pots containing Plantimax® substrate and cultivated under photoperiod of 14 h illumination and light intensity of 120 μmol m^{-2} s^{-1} for 15 days. After this, the plants were transplanted into 20 L pots and cultivated in green house for 3–4 months. Completely expanded and non-senescent leaves of non-flowering were harvested pre-dawn for preparation of epidermal fragments as described next.

Guard cell-enriched epidermal fragment preparation

The epidermal fragments were prepared pre-dawn in order to simulate the circadian clock of the stomatal opening observed *in vivo*, given that a fast stomatal opening is observed in early morning in plants growing under tropical conditions (Antunes *et al*. 2012). The preparation of guard cell-enriched epidermal fragments was performed according to the method proposed by Kruse *et al*. (1989) and adapted for tobacco. The leaves were blended for 3 min (three pulses of 1 min) in a Waring blender (Philips, RI 2044 B.V. International Philips, Amsterdam, The Netherlands)) fitted with an internal filter in order to isolate epidermal fragments from mesophyll cells and fibres. Microscopic analysis revealed that the filter used was essential in order to obtain high purity of the guard cell-enriched epidermal fragments. After isolation, guard cell-enriched epidermal fragments were collected on a nylon membrane and thoroughly washed with 1.5–2.0 L of deionized water in order to remove contaminants including both pavement and palisade cell debris that might be present together with the epidermal fragments. Each preparation required approximately 5 min.

A number of preparations were carried out and a pool of guard cell-enriched epidermal fragments was prepared

pre-dawn and stored in the dark in a hypertonic solution to avoid stomatal opening. This step was necessary in order to collect sufficient material to perform the experiments and for further metabolomic analysis, as well as to avoid stomatal opening that could occur through the removal of backpressure during the process of epidermal fragment preparation. After collecting sufficient material for the experiment, the epidermal fragments were exhaustively washed again to remove the hypertonic solution. Experiments were started by transferring guard cell-enriched epidermal fragments to solutions enriched with potassium (KCl) and/or sucrose in the light. The preparation protocol results in guard cell purity of 98% (Antunes *et al*. 2012). The viability of the guard cells was analysed by staining with fluorescein diacetate and propidium iodide dyes as described in Huang *et al*. (1986), which showed that the only living cells in the epidermal fragments are guard cells. After the last preparation, a sample was analysed under a light microscope to measure the stomatal aperture and another was washed extensively and frozen as control.

The concentration of all solutions was selected based on the literature regarding light-induced stomatal opening experiments as well as kinetic data for the guard cell sucrose transporter (Outlaw 1995). All solutions were corrected to pH 6.5 and a final volume of 10 mL, and were composed as follows:

- Control (MES/NaOH 5 mM + $CaCl_2$ 50 μM + mannitol 30 mM)
- KCl (MES/NaOH 5 mM + $CaCl_2$ 50 μM + mannitol 20 mM + KCl 5 mM)
- Sucrose (MES/NaOH 5 mM + $CaCl_2$ 50 μM + mannitol 10 mM + sucrose 20 mM)
- KCl and sucrose (MES/NaOH 5 mM + $CaCl_2$ 50 μM + KCl 5 mM + sucrose 20 mM)

The solutions used in the feeding experiment with $NaH^{13}CO_3^-$ were as described earlier but with the addition of 5 mM of $NaH^{13}CO_3^-$ to each treatment. For the experiments spanning the time from 0 to 40 min, an initial sample was collected on a membrane (200 μM), washed extensively and frozen for metabolite analysis. This sample corresponds to time 0 in the figures. Immediately after placing the guard cell-enriched epidermal fragments in the solutions, a sample was collected and stomatal aperture was measured. Another sample was then collected on a membrane, washed extensively and frozen which corresponds to time 1 in the figures. For the feeding experiment with $NaH^{13}CO_3^-$, the samples were not washed before freezing in order to avoid changes in the metabolism that may result from washing. For this reason, we did not determine the level of sucrose in the treatments that contain sucrose in the medium.

Stomatal aperture measurements

After preparation of guard cell-enriched epidermal fragments, a sample was separated and analysed using a light microscope (Carl Zeiss, Axiostar Plus, Göttingen, Germany) with a coupled digital camera. Stomatal aperture was measured for at least 40 stoma per treatment from several different epidermal fragments and recorded as the width of stomatal pore or as the length multiplied by the width of stomatal pore using Image Pro Plus® software, Media Cybernetics, Inc., Rockville, Maryland. The data obtained were compared as described in Statistical analyses section.

Extraction and analysis of metabolites

The metabolite extraction for gas chromatography-coupled time of flight mass spectrometry (GC-TOF-MS) and sugar/starch quantification by spectrophotometric assays was performed according to Lisec *et al*. (2006). Approximately 20 mg of lyophilized guard cell-enriched epidermal fragments was disrupted by shaking with metal balls and extracted using 1000 μL of methanol (100%) at 70 °C for 1 h with constant agitation. For GC-TOF-MS analysis, 60 μL of ribitol (0.2 mg mL^{-1} stock in dH_2O) was added as an internal quantitative standard. The extract was centrifuged at 11 000 *g* for 10 min, and 600 μL of the supernatant was transferred to another tube, where 500 μL of chloroform (100%) (liquid chromatography grade, Sigma, Munich, Germany) and 800 μL of deionized water were added. After vortexing for 10 s, another centrifugation was carried out for 15min at 2200 *g*. A total of 1000 μL of polar (upper) phase was collected and transferred to 1.5 mL tubes, and dried in a vacuum concentrator. For GC-TOF-MS analysis, the sample derivatization was carried out according to Lisec *et al*. (2006) through *N*-methyl-N-(trimethylsilyl) trifluoroacetamide (MSTFA; CAS 24589-78-4, Macherey & Nagel, Düren, Germany) and methoxyamine hydrochloride (CAS 593-56-6, Sigma) dissolved at 20 mg mL^{-1} in pure pyridine (CAS 110-86-1, Merck, Darmstadt, Germany). The GC-TOF-MS metabolite determinations were quantified as described in Roessner-Tunali *et al*. (2001). The metabolite reporting guidelines and the overview of the metabolite reporting list are shown in Supporting Information Dataset S1. The fractional enrichment of metabolite pools was determined exactly as described previously by Roessner-Tunali *et al*. (2004) and label redistribution was expressed as per Studart-Guimarães *et al*. (2007). The analysis of relative abundance of mass isotopomers was carried out using Xcalibur 2.1 software (Thermo Fisher Scientific, Waltham, MA, USA) and CORRECTOR program as described in Huege *et al.* (2014).

Sugars and starch quantification

The levels of soluble sugars (sucrose, fructose and glucose) as well as starch were measured spectrophotometrically using a microplate spectrophotometer (Tunable Microplate Reader, VERSAmax, Sunnyvale, CA, USA) as detailed in Trethewey *et al*. (1999). The metabolite extraction was performed as described earlier with no addition of ribitol. The polar (upper) phase previously dried in a speed vacuum was resuspended in 150 μL of deionized water and further analysed by sequential enzymatic reactions using HEPES/KOH pH 6.9 (50 mM) as buffer and NAD (2 mM), ATP (1 mM), glucose-6 phosphate-dehydrogenase (2 U

reaction^{-1}), hexokinase (1 U reaction^{-1}), phosphoglucoisomerase (1 U reaction^{-1}) and invertase (Inv; 5 U reaction^{-1}). The level of the metabolites was determined by following the formation of NADH (340 nm) and quantified according to standard curves of glucose (1 mm), fructose (1 mm) and sucrose (1 mm).

Sugar levels in the medium from epidermal fragment experiments (Supporting Information Fig. S3) were quantified by collecting 200 μL of the medium per time point and using 50 μL in the assays. The reaction mixture for sugar quantification was the same as described earlier. However, the calculations were carried out using standard curves for sucrose, glucose and fructose constructed from stock solutions of 0.1 mm. We decided to use a standard curve instead of the molar extinction coefficient of NADH for these assays as it permits a more critical assessment of the noise of the assay and limits of detection. The values measured in the samples collected from the medium are comparable with the limit of detection showed by the standard curves.

Starch was measured in the insoluble residue remaining after the methanolic extraction described earlier. The pellet of the methanolic extraction was rinsed three times with ethanol (80%) at 70 °C and starch was then solubilized using 400 μL of KOH (0.2 m) at 90 °C for 1 h. After neutralization with 70 μL of acetic acid (1 m), 100 μL of this solution was used for starch digestion using citrate buffer (0.3 m) (pH 5.0) and amyloglucosidase (1 U reaction^{-1}) at 55 °C for 1 h in a final volume of 300 μL. The starch level was then determined as glucose hydrolysed from starch by amyloglucosidase using the procedure described earlier for glucose quantification.

Enzyme activities

Extracts of whole leaves and guard cell-enriched epidermal fragments were prepared according to Gibon *et al*. (2004) except that Triton X-100 was used at a concentration of 1% and glycerol at 20% (vol/vol). Enzyme activities of sucrose synthase (SuSy) (EC 2.4.1.13) in the direction of sucrose breakdown and Inv (EC 3.2.1.26) were performed according to Zrenner *et al*. (1995). For SuSy activity, the protein extract was incubated in reaction mixture containing HEPES/KOH pH 7.4 (20 mm), sucrose (0.4 m) and UDP (2 mm) for 40 min at 25 °C. The reaction was stopped by heating to 95 °C for 3 min. The UDP glucose produced was determined spectrophotometrically using a microplate reader (Tunable Microplate Reader, VERSAmax) in a reaction mixture containing glycine pH 8.9 (0.2 m), $MgCl_2$ (5 mm), NAD (2 mm) and UDP glucose dehydrogenase (0.005 U reaction^{-1}). For Invs, the protein extract was incubated in a reaction mixture containing HEPES/KOH pH 7.5 (0.1 m) and sucrose (0.1 m) for alkaline Inv (cytosolic Inv), and sodium acetate pH 4.6 (0.1 m) and sucrose (0.1 m) for acid Inv (vacuolar Inv). Both reactions were stopped by heating to 95 °C for 3 min. The levels of glucose and fructose produced by Inv activities were determined as described earlier.

SuSy activity in the direction of sucrose breakdown was also determined in desalted extracts and expressed on a per protein basis (nmol UDPG min^{-1} μg protein^{-1}). The total protein content of the extract was determined according to Bradford (1976). The protein extract was desalted using gel filtration chromatography according to Stitt *et al*. (1989). The reaction mixture and the UDP glucose quantification was performed exactly as described earlier.

Statistical analyses

The values obtained for each treatment were statistically compared using Student's *t*-test ($P < 0.05$) when there was only one time point. The data from the experiments for which there was more than one time point were analysed using an analysis of variance (ANOVA) followed by posterior Dunnett's test ($P < 0.05$) in order to determine the effect of time, treatment and interaction of both time and treatment. All statistical analyses were performed using SAEG system version 9.0 (Fundação Arthur Bernardes, Viçosa, Brazil).

RESULTS

Experimental set-up for *in vivo* guard cell analyses

Several studies have compared the transcriptome (Leonhardt *et al*. 2004; Yang *et al*. 2008; Bates *et al*. 2012), proteome (Zhao *et al*. 2008; Zhu *et al.* 2009, 2010, 2014) and most recently metabolome (Jin *et al*. 2013) of guard cells with mesophyll cells with the principal focus being responses mediated by abscisic acid. However, a caveat to these studies is that the majority were carried out using protoplasts which, while an effective experimental system, may not reflect the situation *in planta*. We therefore analysed changes in guard cell metabolism during light-induced stomatal opening using guard cell-enriched epidermal fragments for several reasons: (1) unlike protoplast isolation, epidermal fragment preparation maintains the cell wall of the cells intact as well as the intercellular spaces between guard cells and the pavement cells, where it is known that the accumulation of metabolites has a great influence on stomatal movements *in vivo* (Lu *et al*. 1995, 1997; Kang *et al*. 2007; Araújo *et al*. 2011b); (2) epidermal fragment preparation is faster than guard cell protoplast isolation that can require over 5 h to carry out, which is too long to isolate and initiate experiments and still respect the circadian rhythm of stomatal movements; and (3) it allows measurements of stomatal aperture that cannot be made in protoplast preparations. Thus, although the guard cells in epidermal fragments are still separated from the mesophyll cells, we consider this experimental system to be closer to the situation observed *in planta* than that of protoplasts.

As a first step we optimized the methodology for the isolation and collection of sufficient guard cell material for metabolomic analysis during stomatal opening. To this end, at least six experiments were carried out. In each experiment, guard cell-enriched epidermal fragment preparations were carried out over a maximum of 2 h using approximately 100 fully expanded leaves (leaf area ~0.4 m^2) from at least 30 tobacco plants. The preparation of guard cell-enriched epi-

dermal fragments was carried out pre-dawn in order to harvest guard cells with the stomatal pore closed and to minimize light-induced changes in guard cell metabolism. The guard cell-enriched epidermal fragments were thereafter exposed to white light (300 μmol photons m^{-2} s^{-1}). The light source was separated from the epidermal fragment preparations by a water layer in order to avoid simultaneous heating of the samples. The lack of transfer of heat to the samples was confirmed by thermal imaging (Supporting Information Fig. S1a). Immediately following the last preparation and at each time point of the experiment a sample of the guard cell-enriched epidermal fragments was analysed under a microscope in order to measure the stomatal aperture while another sample was collected on a nylon membrane, washed and frozen. Opening of the stomatal pore during incubation indicated that guard cells remained functional after preparation (Supporting Information Fig. S1b,c) and fluorescein diacetate and propidium iodide staining indicated that the preparation method did not result in guard cell death (Supporting Information Fig. S1d).

Changes in soluble sugar content during light- and potassium-induced stomatal opening

Although K^+ is an osmolyte that induces stomatal opening (Andrés *et al*. 2014), and the contribution of sucrose as a substrate during this process has been recently proposed (Antunes *et al*. 2012), the role of sucrose during K^+-induced stomatal opening remains incompletely understood. Thus, in order to analyse the role of sucrose, and its breakdown products, fructose and glucose, as well as starch content during light- and K^+-induced stomatal opening, guard cell-enriched epidermal fragments were incubated in a solution containing K^+ (KCl) in the light and samples were collected over 120 min. Stomatal aperture increased dramatically from 0 to 40 min but to a far lesser extent during extended incubation periods (Fig. 1a). No difference was observed in stomatal aperture between the control and K^+ treatment at 40 and 80 min. However, after 120 min the stomatal aperture was greater under K^+ treatment than in the control (Fig. 1a). The level of sucrose and glucose was significantly reduced over time in both the control and K^+ treatment, but to a greater extent in the K^+ treatment (Fig. 1b,c). However, the level of

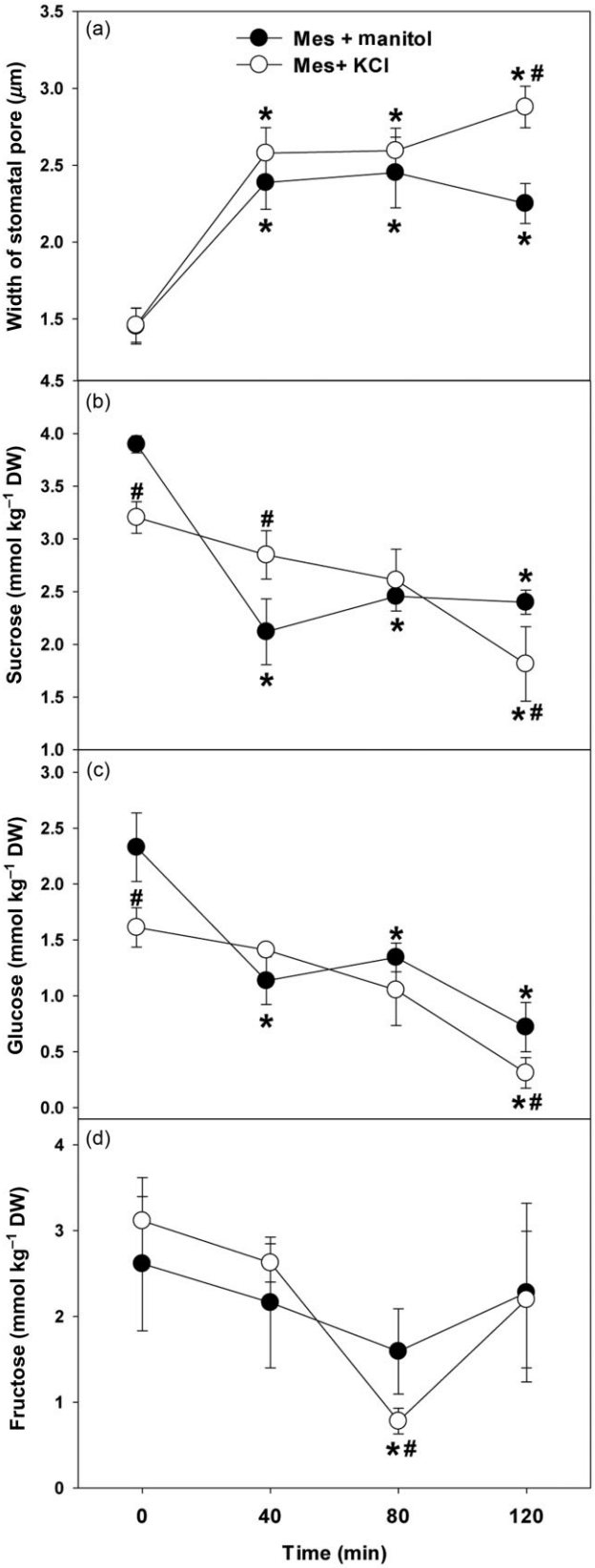

Figure 1. Stomatal aperture (a) and changes in sucrose (b), glucose (c) and fructose (d) content of epidermal fragments during light- and potassium-induced stomatal opening. Guard cell-enriched epidermal fragments were incubated in the light for 0, 40, 80 and 12 min in MES buffer solution (MES + $CaCl_2$ + mannitol) or K^+ solution (MES + $CaCl_2$ + KCl). Stomatal aperture was determined using an optical microscope as the width of the stomatal pore ($n = 40 \pm$ SE) and sugars were quantified by enzymatic method (see Materials and Methods for details) ($n = 4 \pm$ SE). Asterisks indicate values that are significantly different from time 0 by analysis of variance and Dunnett's test ($P < 0.05$). Hash (#) indicates values that are significantly different from control treatment at the same time point by Student's *t*-test ($P < 0.05$).

fructose was unaltered over time, with the exception of the reduction observed at 80 min in the K^+ treatment (Fig. 1d). Decreased sugar content was correlated with increased stomatal aperture (Supporting Information Fig. S2a–d). A linear relationship was observed as the increase in stomatal aperture was accompanied by decreases in sucrose in the control treatment (Supporting Information Fig. S2a). That the decreases in sugars were associated with increases in stomatal aperture raise the question of the fate of sugars: are they metabolized in the guard cell itself or is there an efflux of these sugars from the cell to the apoplast? In order to address this, we carefully analysed the sugar content of medium samples collected during the experiment. The values measured were very low but still above the limit of detection of the method (see Material and Methods for details). Moreover, no differences were detected between these treatments over time (Supporting Information Fig. S3a–c), suggesting that the decrease in sucrose that we observed (Fig. 1) is due to breakdown within the guard cells *per se* and not merely the result of efflux from the cell.

Sucrose metabolism during light-induced stomatal opening in the presence of sucrose in the medium

Given that our first experiment indicated that 40 min was sufficient to induce stomatal opening and changes in sucrose content occurred during this period, we next carried out an experiment within this time frame in order to understand the role of sucrose during light-induced stomatal opening in the presence of sucrose in the medium. Dark-adapted, guard cell-enriched epidermal fragments were incubated in the presence or absence of sucrose and stomatal aperture, sugar and starch contents were analysed. Stomatal aperture increased over time in both control (30 mM mannitol) and sucrose solution (10 mM mannitol + 20 mM sucrose) treatments (Fig. 2a,b). However, this increase was accompanied by changes in sugar content only following the treatment with sucrose. As expected, an increase in sucrose content was observed following sucrose treatment (Fig. 2c). Interestingly, the increase in sucrose was followed by simultaneous increases in fructose and glucose levels (Fig. 2e,g). Compared with t_0 sucrose, fructose and glucose levels had significantly increased after 8, 16 and 16 min, respectively. On the other hand, no significant differences were observed in sucrose, fructose and glucose levels over time in the control (mannitol) treatment (Fig. 2d,f,h). The starch content was invariant over time in both conditions (Fig. 2c,d). Taken together, these results suggest a high sucrolytic capacity of guard cells. However, the route by which sucrose is degraded in guard cells, via SuSy or via Inv, remains rather unclear. Given that the levels of fructose are considerably higher than those of glucose, it is reasonable to assume that a considerable portion of the flux is carried by the SuSy route that does not yield glucose as a direct product. We next evaluated enzymatic activities of SuSy and Inv in whole leaves and in guard cell-enriched epidermal fragments in order to compare the capacity of these enzymes between sample types. Consistent with the aforementioned comment, SuSy activity was higher in guard cells compared with whole leaves (~40-fold and ~27-fold when expressed by fresh weight or protein content, respectively; Fig. 3a,b). By contrast, alkaline Inv and acid Inv activities were ~13-fold and ~10-fold higher, respectively, in whole leaves compared with guard cells (Fig. 3c,d). Furthermore, the ratio between SuSy activity and Inv activity is higher in guard cells than leaves (Fig. 3e,f). SuSy activity was 29% higher than alkaline Inv (Fig. 3f), whereas acid Inv activity is 12-fold higher than SuSy activity in guard cells (Fig. 3e).

Metabolic profile and isotope labelling kinetics in guard cells during dark-to-light transition

Our results indicated that sucrose is broken down in guard cells during stomatal opening. However, the source of sucrose and the fate of carbon derived from sucrose are still unknown. Furthermore, given that the mode of CO_2 fixation and the distribution of the photosynthetic fluxes in guard cells are still poorly understood, we next decided to perform feeding experiments following the supply of ^{13}C-$NaHCO_3^-$ (see Materials and Methods for details). For this purpose, guard cells were incubated with labelled substrate in the light for 40 min and the metabolite profile and ^{13}C enrichment were determined using a well-established GC-TOF-MS platform (Roessner-Tunali *et al.* 2004; Lisec *et al*. 2006; Huege *et al.* 2014) adapted for tobacco epidermal fragment analysis (see Materials and Methods for details). Additionally, we analysed the mass isotopomer distribution of sucrose, aspartate and malate (*m/z* fragments 361, 232 and 233, respectively) in order to verify the possibilities of CO_2 fixation by ribulose-1,5-biphosphate carboxylase/oxygenase (Rubisco) and/or phospho*enol*pyruvate carboxylase (PEPcase). This approach enabled us to identify the fate of the carbon fixed in the light as well as to assess the mode of CO_2 fixation in tobacco guard cells.

In general, levels of metabolites responded significantly to both treatment and time of incubation (Supporting Information Table S1). Rather unexpectedly, many metabolites accumulated over the first 24 min and then decreased until the end of the experiment (Figs 4 & 5; Supporting Information Fig. S4). This pattern occurred independently of the treatment although the magnitude of effect was treatment dependent, with the decrease after 24 min being considerably more pronounced under K^+ treatment. This pattern was observed for the abundance of organic acids, amino acids such as serine, threonine and aspartate, as well as erythritol, threonate, glycerol and nicotinic acid (Figs 4 & 5; Supporting Information Fig. S4). One exception to this was the behaviour of sucrose that decreased significantly under K^+ treatment with levels being significantly lower than the control from 8 to 32 min (Fig. 4). Because of the large amounts of sucrose in the treatment solution, sucrose was not quantified in the treatments containing sucrose. Another exception to the pattern observed for organic and amino acids was that observed for *myo*-inositol, which increased under control and K^+ treatment while decreased under sucrose treatment (Supporting Information Fig. S4).

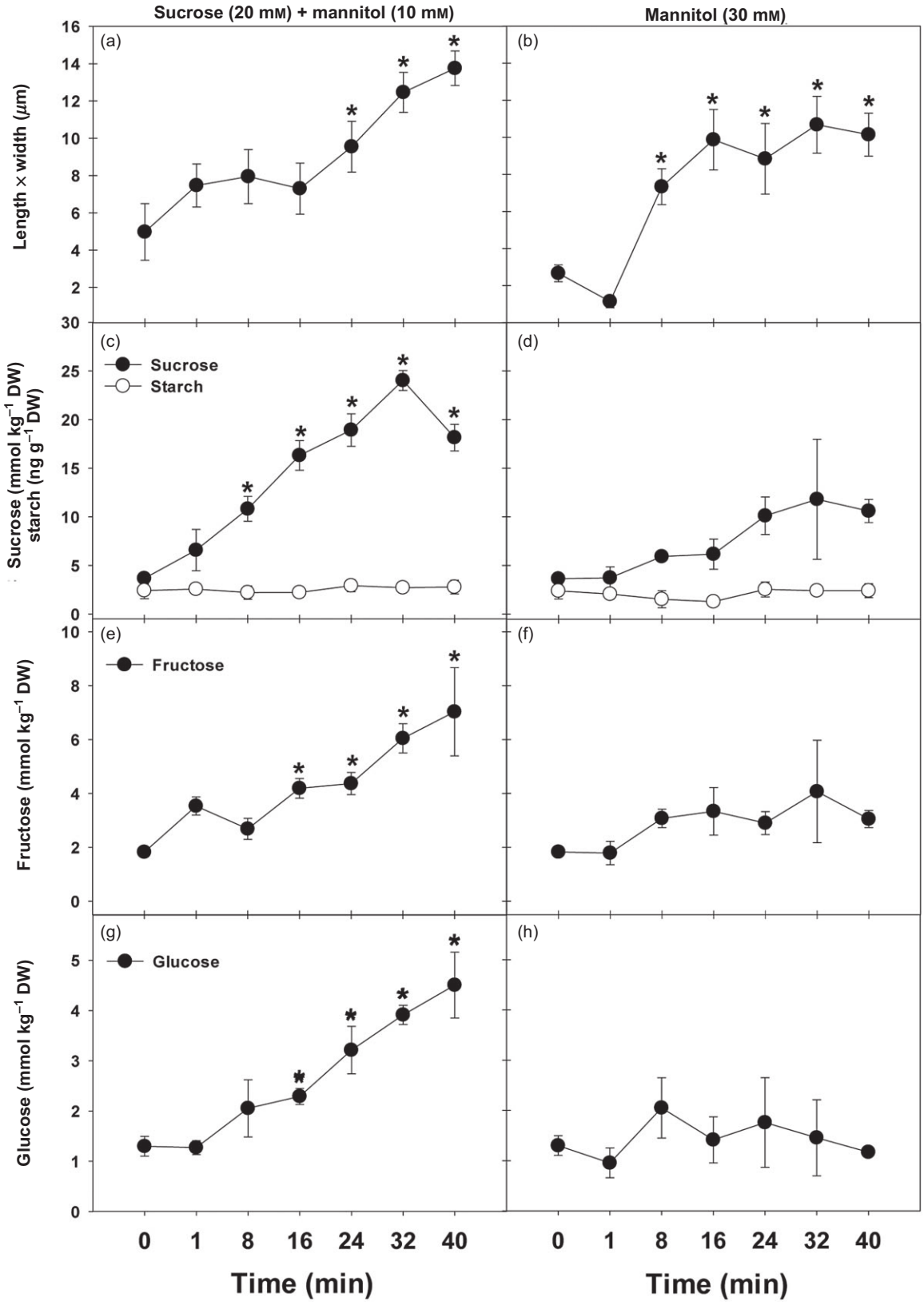

Figure 2. Changes in stomatal aperture (length × width of stomatal pore) and in sucrose, glucose, fructose and starch levels over time. Guard cell-enriched epidermal fragments were incubated in the light spanning the time from 0 to 40 min in mannitol solution (MES + $CaCl_2$ + mannitol) (right panel – b, d, f, h) and sucrose solution (MES + $CaCl_2$ + mannitol + sucrose) (left panel – a, c, e, g). Asterisks indicate values that are significantly different from time 0 by analysis of variance and Dunnett's test ($P < 0.05$) ($n = 4 \pm$ SE).

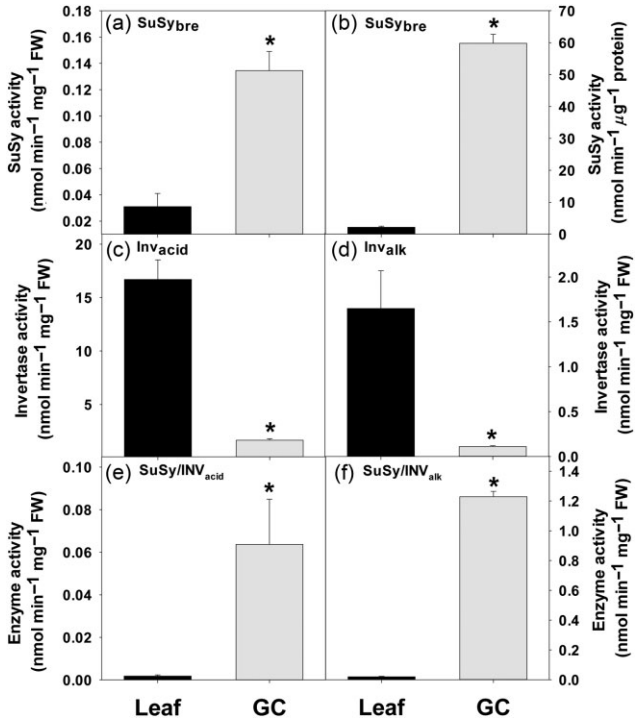

Figure 3. Enzyme activities in guard cell-enriched epidermal fragments and leaves of wild-type *Nicotiana tabacum* L. $SuSy_{bre}$ – sucrose synthase activity in sucrose breakdown direction expressed by fresh weight (nmol UDPG min^{-1} mg^{-1} fresh weight; top left panel) or by protein content (nmol UDPG min^{-1} μg^{-1} protein; top right panel); INV_{aci} – acid invertase activity (INV_{aci}) (nmol glucose min^{-1} mg^{-1} fresh weight); INV_{alk} – alkaline invertase activity (nmol glucose min^{-1} mg^{-1} fresh weight). The data of enzyme activities expressed per fresh weight were used to determine the relationship between SuSy activity for both invertase activities. Asterisks indicate significantly different values by Student's *t*-test ($P < 0.05$) ($n = 5 \pm$ SE).

Concomitant with the decrease in sucrose, we also observed an increase in the levels and ^{13}C enrichment of metabolites of, or associated with, the tricarboxylic acid (TCA) cycle such as malate, fumarate, succinate and glutamate (Figs 4 & 6). Furthermore, although the abundance of serine, threonine and aspartate responded in a similar manner to these metabolites, the abundance of the amino acids alanine, phenylalanine, leucine and isoleucine decreased under K^+ treatment and increased under sucrose treatment over the incubation time (Fig. 5). Pyruvate, glycine and serine tended to increase over time, although the magnitude of this change was higher for pyruvate under K^+, higher for glycine under sucrose and lower for serine under K^+ and sucrose (Fig. 5). Similarly, the level of glycerate and glycolate increased over time in all treatments with a linear tendency under sucrose treatment (Supporting Information Fig. S4).

The ^{13}C enrichment of sucrose and metabolites of, or associated with, the TCA cycle also responded during the incubation period. An increase in sucrose ^{13}C enrichment over time occurred under both control and K^+ treatment, but this occurred to a greater extent under K^+ treatment after 32 min (Fig. 6). An increase in aspartate ^{13}C enrichment over time occurred but to a greater extent under the control treatment (Fig. 6). The ^{13}C enrichment in malate and fumarate was lower in the presence of sucrose compared with the K^+ treatment whereas glutamate and succinate were labelled similarly under sucrose and K^+ treatments but to a greater extent in the sucrose treatment at 16 min (Fig. 6).

Analysis of mass isotopomer abundances revealed that specific fragments of sucrose, aspartate and malate were fully labelled; the ions *m/z* 367 (sucrose *m6*), *m/z* 235 (aspartate *m3*) and *m/z* 236 (malate *m3*) were detected by GC-MS indicating the presence of the maximum possible (six, three and three, respectively) number of ^{13}C atoms in these metabolite fragments (Fig. 7a–c). The abundance of the mass isotopomers sucrose *m6* (*m/z* 367) and malate *m3* (*m/z* 236) increased over time to a greater extent in the K^+ treatment, whereas the mass isotopomer aspartate *m3* (*m/z* 235) also increased over time but to a greater extent in the control treatment after 32 min (Fig. 7d–f), consistent with the ^{13}C enrichment (%) observed in these metabolites (Fig. 6). The detection of significant levels of the sucrose *m6* and aspartate *m3* mass isotopomers excludes the possibility that guard cells are fixing CO_2 exclusively by PEPcase (Fig. 8a) and provides evidence for simultaneous CO_2 fixation by both Rubisco and PEPcase (Fig. 8b). Overall the results indicate that sucrose levels decrease during both light- and K^+-induced stomatal opening and that this occurs with a concomitant increase in the level and ^{13}C enrichment of metabolites of, or associated with, the TCA cycle (Fig. 9).

DISCUSSION

Our current understanding of guard cell metabolism is largely informed by studies carried out in the 1970s and 1980s using radiolabelled precursors that provided initial information regarding metabolic fluxes in guard cells (Willmer & Dittrich 1974; MacRobbie 1981; Brown & Outlaw 1982). The current widespread availability of mass spectrometry technologies and ^{13}C-labelled precursors coupled with modelling approaches has significantly improved our understanding of the dynamics of metabolic networks of different cell types and organisms (Fernie & Morgan 2013; Heise *et al*. 2014). However, to our knowledge, stable isotope labelling experiments with analysis of label distribution using mass spectrometry have not yet been applied to the investigation of guard cell metabolism. For this reason, we adjusted a methodology to work with physiologically intact guard cells and used this technique in combination with metabolite profiling to provide novel information regarding guard cell metabolism during light-induced stomatal opening and provide further support for our recently postulated role of sucrose as a respiratory substrate supporting stomatal function (Antunes *et al*. 2012).

Do tobacco guard cells fix CO_2 by both Rubisco and PEPcase?

Although a few species do not contain chloroplasts in their guard cells, it is now widely accepted that Calvin–Benson

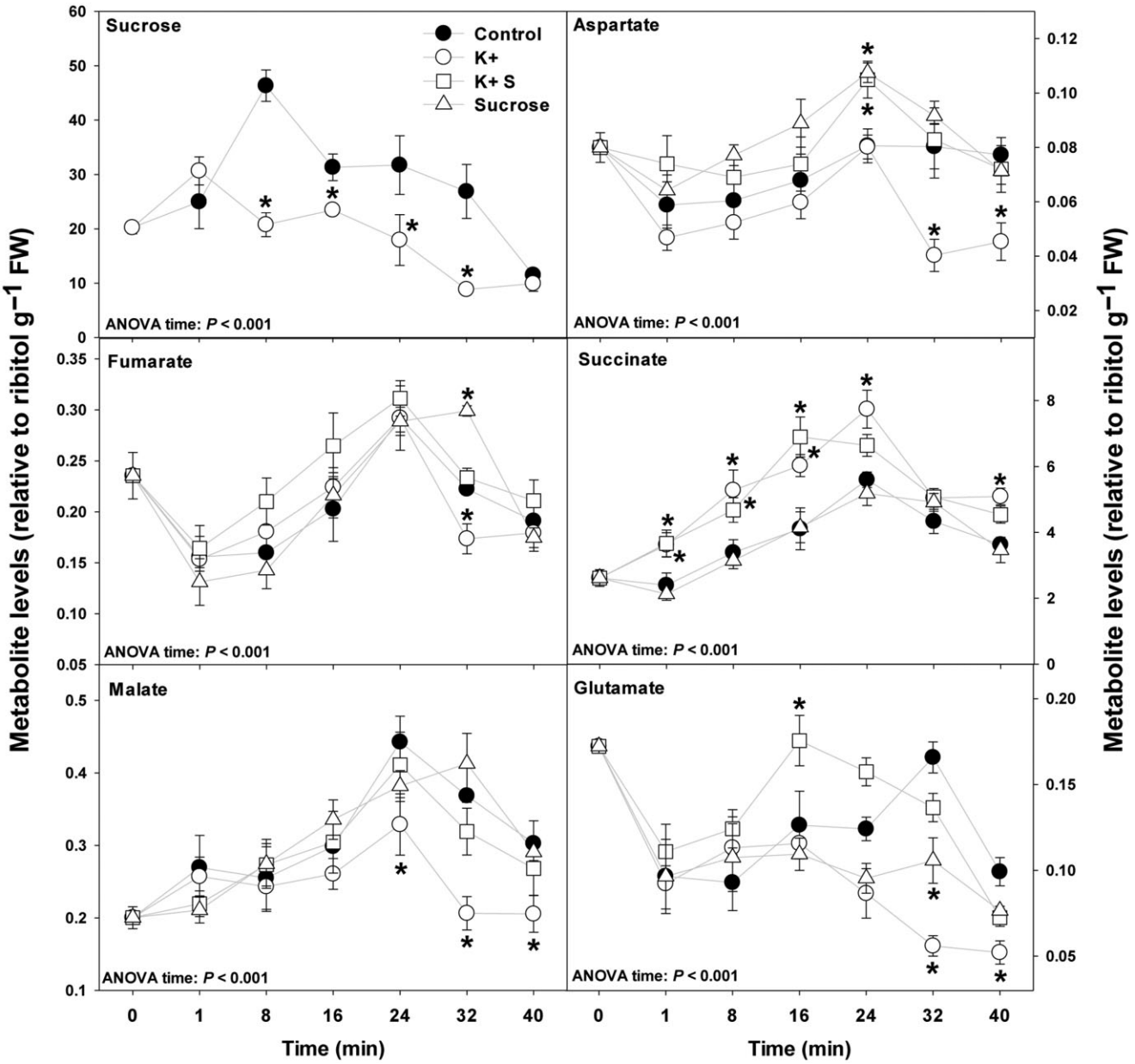

Figure 4. Metabolite levels (relative to ribitol g^{-1} of fresh weight – FW) in guard cell-enriched epidermal fragment of *Nicotiana tabacum*. Control, MES + $CaCl_2$ + mannitol; K^+, MES + $CaCl_2$ + KCl; K^+ + S, MES + $CaCl_2$ + KCl + sucrose; sucrose, MES + $CaCl_2$ + sucrose. Because of the large amounts of sucrose in the treatment solution, sucrose was not quantified in the treatments containing sucrose. Data presented are mean ± SE ($n = 4$). The significance of the influence of both time and treatment in the level of each metabolite was analysed by analysis of variance (ANOVA) and Dunnett's test and is shown in Supporting Information Table S1. Asterisks indicate values that are significantly different from the control treatment at the same time point by ANOVA and Dunnett's test ($P < 0.05$).

cycle enzymes are present in guard cell chloroplasts (Lawson & Blatt 2014; Lawson *et al.* 2014). Moreover, guard cells contain all the machinery necessary for operation of two routes of CO_2 fixation – those catalysed by Rubisco and PEPcase (Outlaw & Manchester 1979; Outlaw *et al.* 1979; Tarczynski *et al.* 1989; Parvathi & Raghavendra 1997; Zeiger *et al.* 2002; Outlaw 2003; Suetsugu *et al.* 2014; Wang *et al.* 2014). However, the mode of CO_2 fixation and hence the relative contribution of the Calvin–Benson cycle to stomatal function is still unclear (Lawson 2009). On the one hand, based on the fact that guard cells have fewer and smaller chloroplasts, low chlorophyll content and relatively low levels of Rubisco, it seems likely that guard cells do not fix significant quantities of CO_2 using Rubisco, suggesting that the Calvin–Benson cycle would not contribute significantly to the overall carbon balance of these cells (Outlaw 1989; Vavasseur & Raghavendra 2005). In contrast Zeiger and co-workers showed that photosynthetic carbon assimilation within guard cells can produce osmotically active sugars (Tallman & Zeiger 1988; Talbott & Zeiger 1993; Zeiger *et al.*

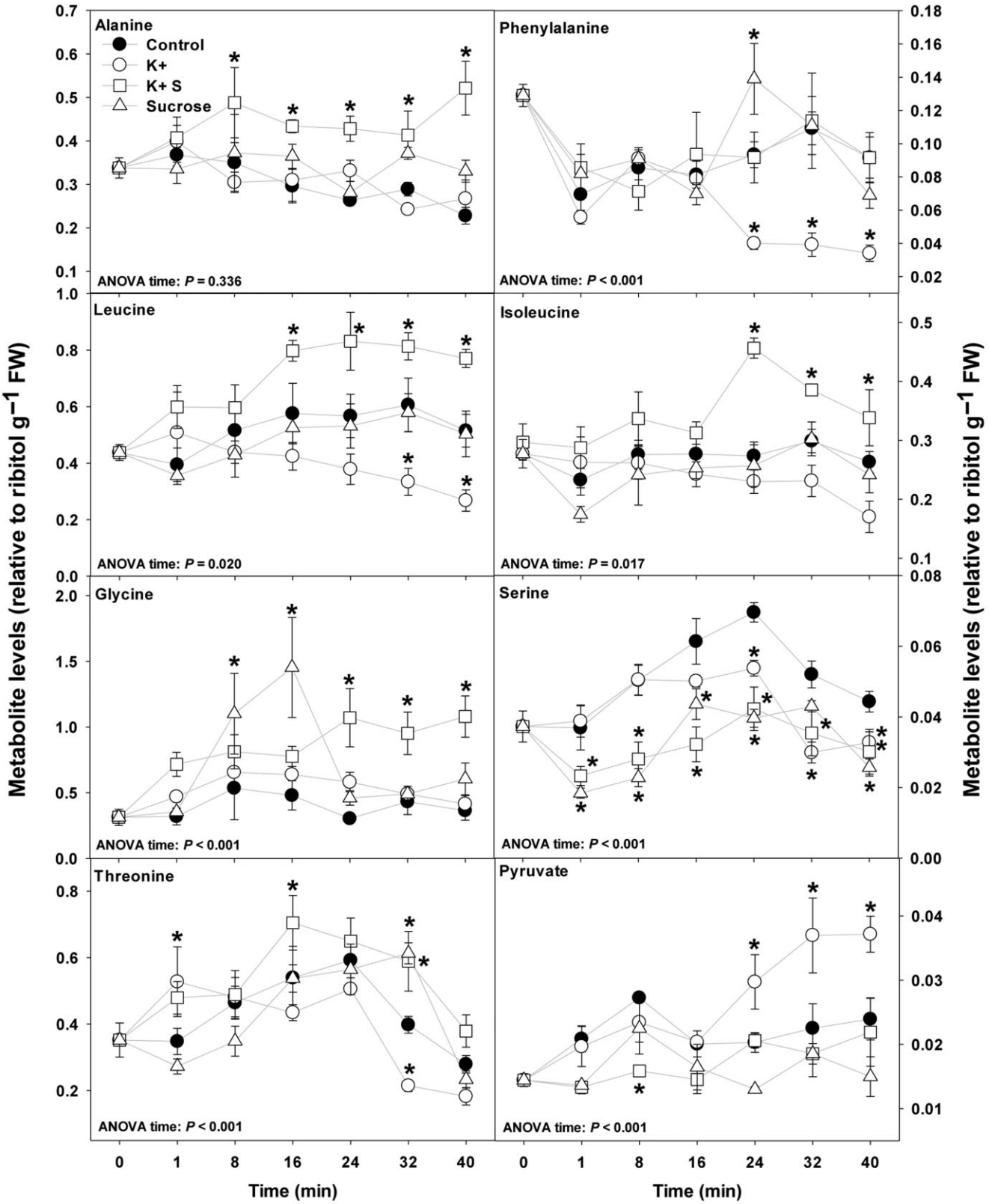

Figure 5. Metabolite levels (relative to ribitol g^{-1} of fresh weight – FW) (relative to time 0) in guard cell-enriched epidermal fragment of *Nicotiana tabacum*. Control, MES + $CaCl_2$ + mannitol; K^+, MES + $CaCl_2$ + KCl; K^+ + S, MES + $CaCl_2$ + KCl + sucrose; sucrose, MES + $CaCl_2$ + sucrose. Data presented are mean ± SE ($n = 4$). The significance of the influence of both time and treatment in the level of each metabolite was analysed by analysis of variance (ANOVA) and Dunnett's test and is shown in Supporting Information Table S1. Asterisks indicate values that are significantly different from the control treatment in the same time point by ANOVA and Dunnett's test ($P < 0.05$).

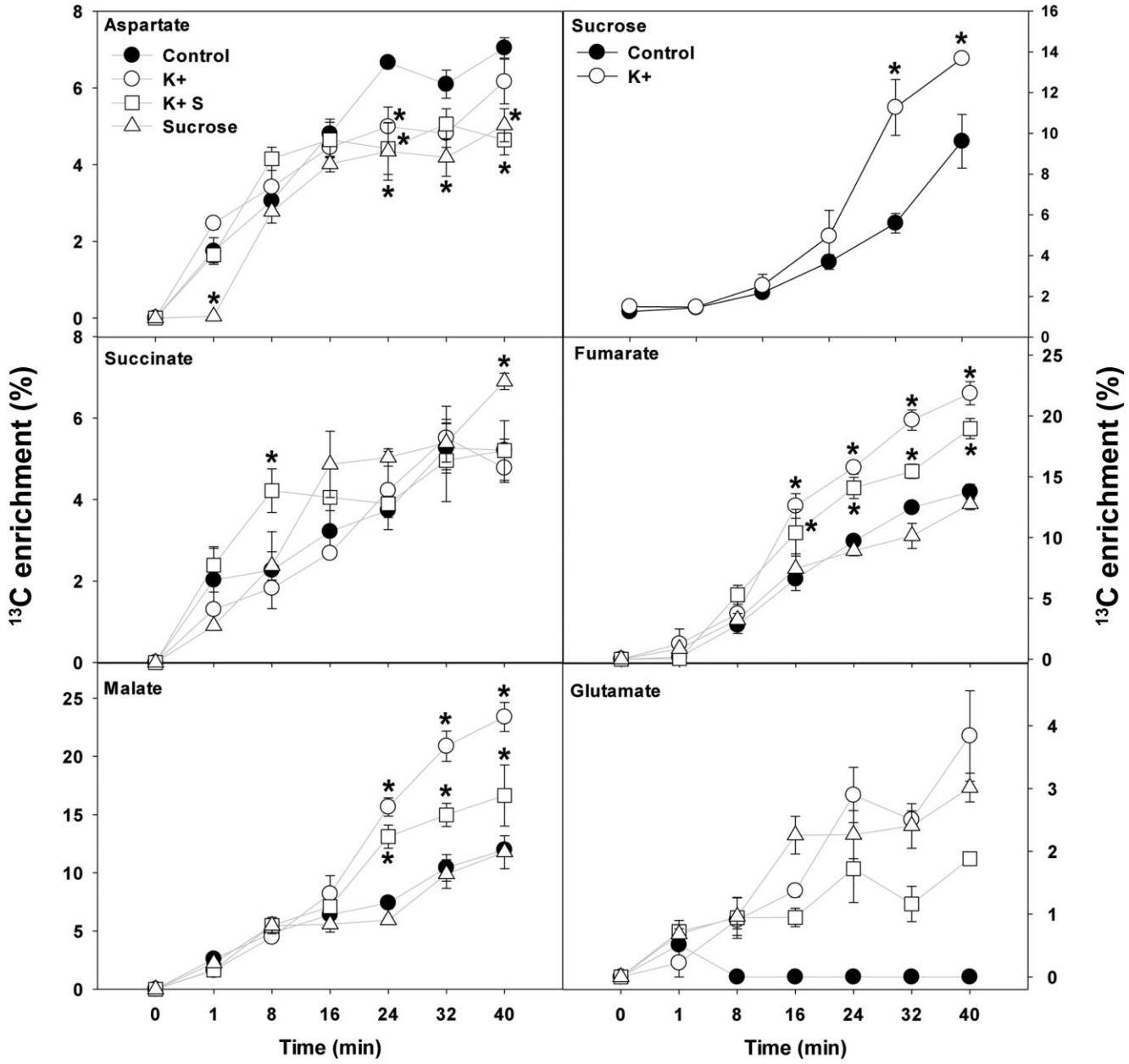

Figure 6. Redistribution of the percentage of ^{13}C label enrichment in metabolites following incubation of guard cell-enriched epidermal fragment of *Nicotiana tabacum*. Guard cell-enriched epidermal fragments were harvested at pre-dawn and fed with ^{13}-$NaHCO_3$ solution in the light under four solutions: control, MES + $CaCl_2$ + mannitol; K^+, MES + $CaCl_2$ + KCl; K^+ + S, MES + $CaCl_2$ + KCl + sucrose; sucrose, MES + $CaCl_2$ + sucrose. Data presented are mean ± SE ($n = 4$). The significance of the influence of both time and treatment in the ^{13}C enrichment in each metabolite was analysed by analysis of variance (ANOVA) and Dunnett's test and is shown in each figure through *P*-values. Given that glutamate was not detected in control samples, statistical analysis was not carried out for this metabolite. Because of the large amounts of sucrose in the treatment solution, sucrose was not quantified in the treatments containing sucrose. Asterisks indicate values significantly different from the control treatment in the same time point by ANOVA and Dunnett's test ($P < 0.05$).

2002). Here, we provide further compelling evidence indicating that tobacco guard cells fix CO_2 using both Rubisco and PEPcase.

The ^{13}C labelling of sucrose when epidermal fragments were incubated in the presence of ^{13}C-$NaHCO_3^-$ suggests CO_2 fixation via Rubisco. However, incorporation of ^{13}C into sucrose could also occur via a route involving PEPcase, phospho*enol*pyruvate carboxykinase (PEPk) and conversion of PEP to sucrose via gluconeogenesis (see dashed blue lines in Fig. 9). Although this second route may operate, it appears unlikely to explain the degree of labelling of sucrose that we encountered as, following our thinking, this route should permit the incorporation of a maximum of two ^{13}C atoms per hexose moiety in sucrose (Fig. 8a). However, our data

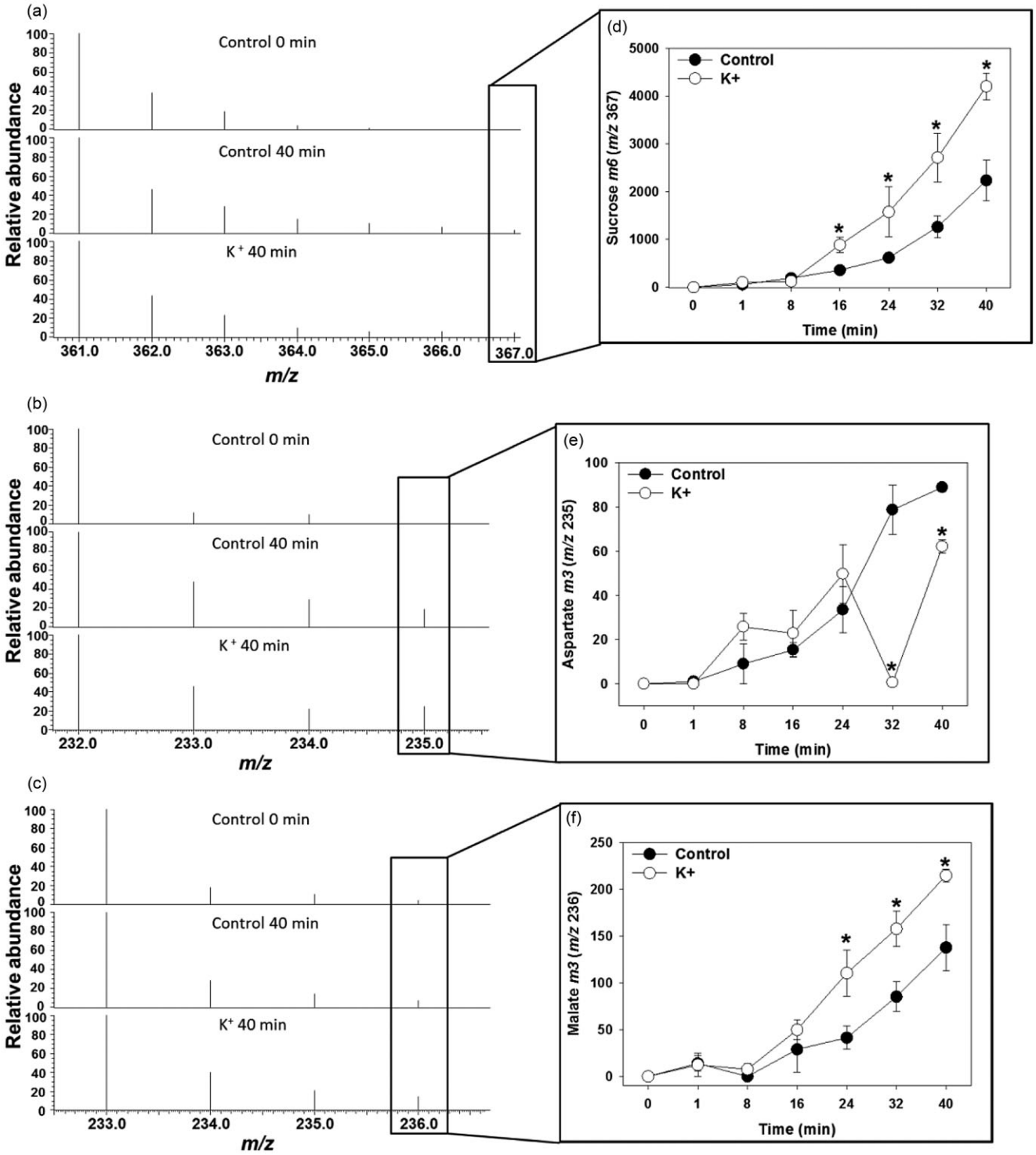

Figure 7. Increase in the abundance of mass isotopomers of sucrose, aspartate and malate. (a–c) Mass spectra showing the relative abundance of mass isotopomers of sucrose (a), aspartate (b) and malate (c) in the control treatment at 0 and 40 min and in the K^+ treatment at 40 min. The abundance of isotopomers is relative to the abundance of the parent ion (*m/z* 361 for sucrose; *m/z* 232 for aspartate; *m/z* 233 for malate). (d–f) The abundance of mass isotopomers sucrose *m6* (*m/z* 367), aspartate *m3* (235 *m/z*) and malate *m3* (236 *m/z*) over time. Treatments and description of the experiment are the same as in Fig. 6. Because of the large amounts of sucrose in the treatment solution, sucrose was not quantified in the treatments containing sucrose. Asterisks indicate values that are significantly different from the control treatment at the same time point by Student's *t*-test ($P < 0.05$).

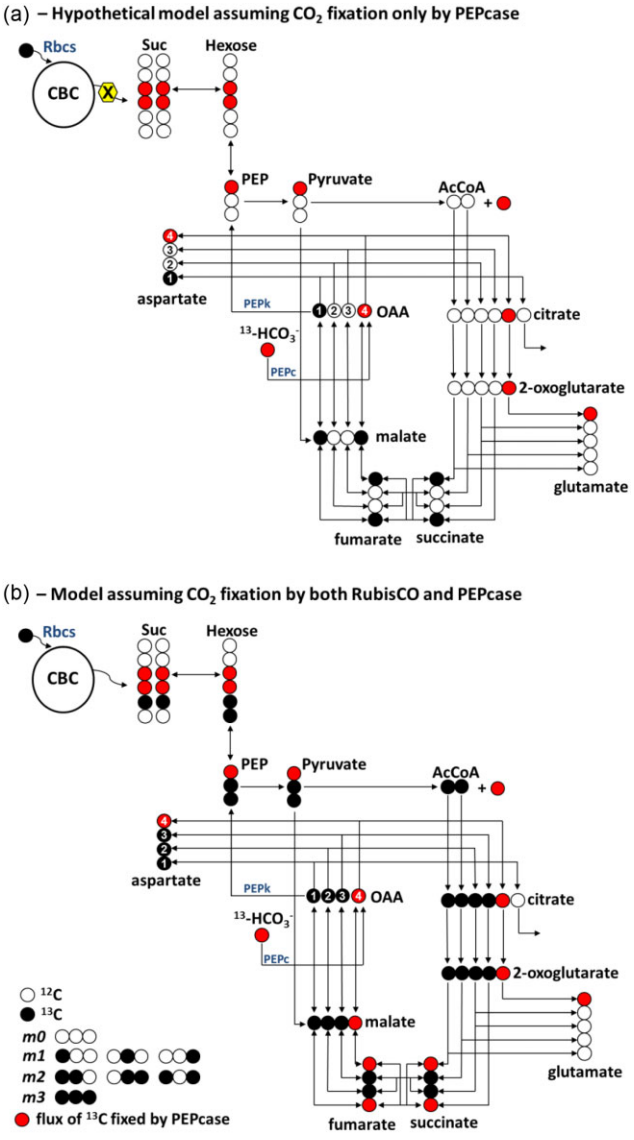

Figure 8. Schematic representation of stable isotope redistribution in guard cells during isotope labelling kinetic experiments. Given the controversies observed in the literature concerning the contribution of the Calvin–Benson cycle (CBC) to stomatal function, we considered the distribution of ^{13}C taking into account CO_2 fixation only by PEPcase (a). However, the label observed in sucrose (*m6* mass isotopomer), aspartate (*m3*) and malate (*m3*) is not compatible with this hypothetical model. Thus, a reasonable model supported by our data is assuming CO_2 fixation by both Rubisco (Rbcs) and PEPcase (b). Small spheres represent carbon atoms (black ^{13}C; white ^{12}C; red ^{13}C fixed by PEPcase). Black spheres in panel (a) represent reflux of the carbon fixed by PEPcase. The abundance of the mass isotopomers observed in the isotope labelling experiment is represented as *m0*, *m1*, *m2* and *m3*, as exemplified in the legend of the figure for a hypothetical metabolite of three carbons. The key enzymes involved in the labelling discussed in the text are shown in blue. PEPc, phospho*enol*pyruvate carboxylase; PEPk, phospho*enol*pyruvate carboxykinase; Rbcs, ribulose-1,5-biphosphate carboxylase/oxygenase.

indicate the incorporation of at least six atoms (Fig. 7a,d), which does not support the occurrence of the hypothetical model assuming CO_2 fixation only by PEPcase (Fig. 8a). Furthermore, fixation by Rubisco is also suggested by the abundance of the aspartate *m3* mass isotopomer; regardless of the number of turns of the TCA cycle, it is not possible to incorporate more than two ^{13}C atoms into aspartate if fixation only through PEPcase is considered (Fig. 8a). The labelling of aspartate *m3* also suggests CO_2 fixation via Rubisco and PEPcase (Fig. 8b) and the direction of a proportion of this fixed carbon to the TCA cycle.

The operation of PEPcase in addition to Rubisco is suggested by the fact that the enrichment of malate and fumarate increased to a much greater extent than that of succinate during the labelling experiment (Fig. 6). This is consistent with label initially being incorporated into OAA through PEPcase (see red spheres in Fig. 8b), followed by the production of labelled malate and fumarate through the reversible reactions catalysed by malate dehydrogenase and fumarase (see black spheres in Fig. 8b). Thus, it seems likely that in tobacco guard cells PEPcase is responsible for the incorporation of at least one ^{13}C into aspartate and metabolites of the TCA cycle through the fixation of ^{13}-HCO_3^- (see red spheres in Fig. 8b). Collectively, the data from the stable isotope kinetic labelling experiment provide novel evidence concerning the mode of CO_2 fixation in guard cells and reveal a simultaneous CO_2 fixation by Rubisco and PEPcase.

The hypothesis of a simultaneous CO_2 fixation by Rubisco and PEPcase is supported by the fact that although guard cells exhibited high rates of CO_2 fixation in the dark compared with mesophyll cells, which suggest higher CO_2 fixation by PEPcase, these rates increased around 50% in the light (Gautier *et al.* 1991), indicating that CO_2 fixation processes were stimulated by light most probably via Rubisco (Outlaw & Manchester 1979; Outlaw *et al.* 1979; Tarczynski *et al.* 1989). Probably not only PEPcase but also the Calvin–Benson cycle plays a positive role during stomatal opening particularly in circumstances wherein the alternate pathway is restricted (Parvathi & Raghavendra 1997). As previously highlighted (Zeiger *et al.* 2002), controversies surrounding the CO_2 fixation by guard cells may arise due to the complexity of guard cell metabolism rather than a lack of data. Although our data do not enable us to categorically distinguish what type of metabolism tobacco guard cells present, the labelling observed in metabolites such as succinate, fumarate and glutamate (which were weakly labelled in rosette tissue of *Arabidopsis*), as well as the faster ^{13}C enrichment in malate compared with whole rosette of *Arabidopsis* (Szecowka *et al.* 2013), supports the hypothesis that guard cells, even those from C3 plants, exhibit similarities to cells with C4 metabolism or CAM (Cockburn 1983; Outlaw 2003; Vavasseur & Raghavendra 2005; Lawson & Blatt 2014; Lawson *et al.* 2014).

Sucrose as substrate for guard cell regulation

Sucrose has long been described as an osmolyte involved in guard cell regulation and consequently stomatal movements

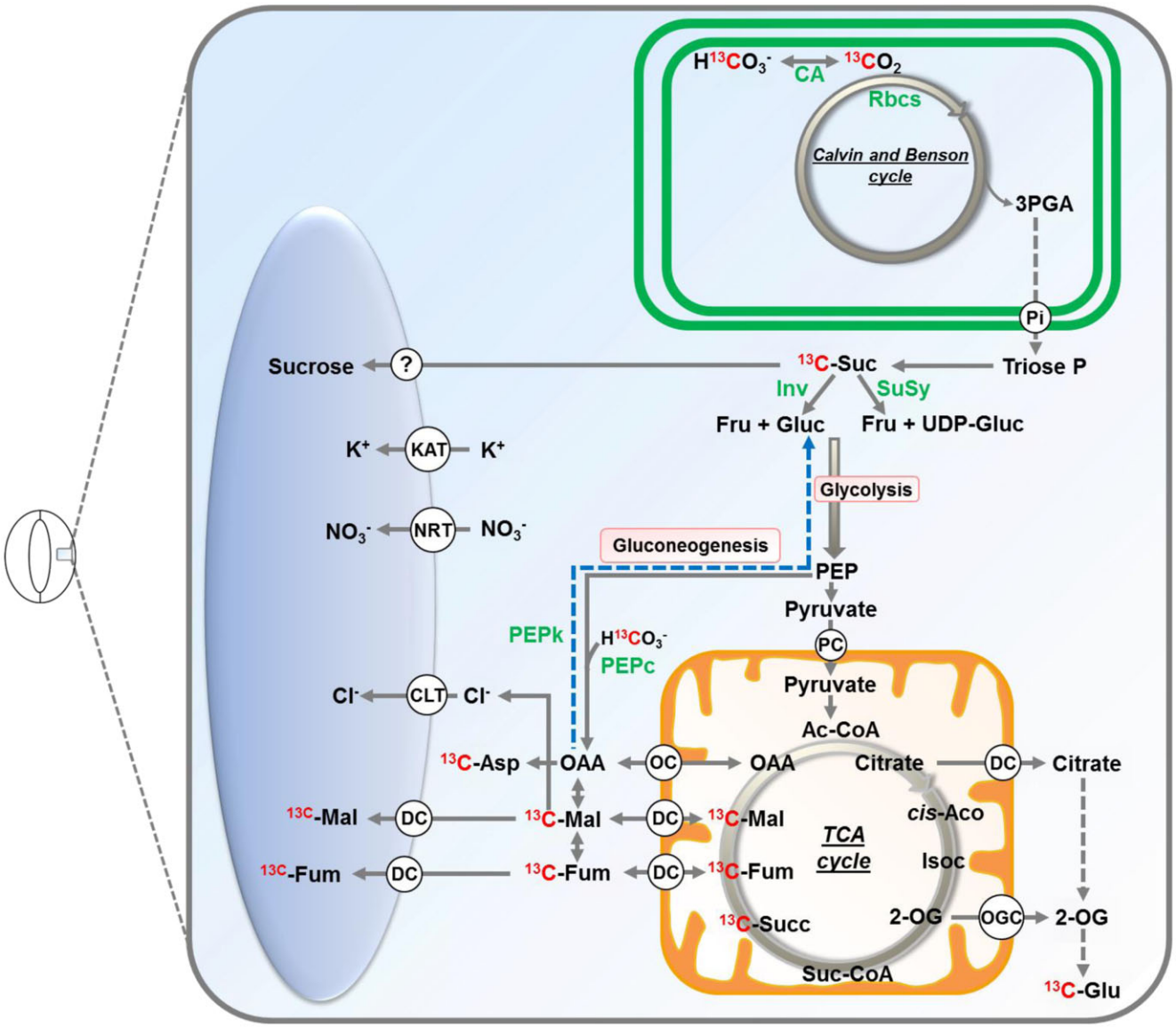

Figure 9. Schematic representation summarizing the changes in guard cell metabolism during light-induced stomatal opening that we observed. The content of sucrose decreased during light- and K^+-induced stomatal opening, whereas starch content does not change. Although the ^{13}C can be incorporated into sucrose via gluconeogenesis (blue dashed lines), the ^{13}C enrichment observed in sucrose is evidence of CO_2 fixation via Rubisco action; however, a simultaneous CO_2 fixation by PEPcase may occur given that ^{13}C enrichment was also observed in malate and aspartate. The ^{13}C enrichment observed in malate, fumarate, succinate and glutamate is substantial evidence that the tricarboxylic acid (TCA) cycle is operating during light-induced stomatal opening. Subcellular compartments are indicated by colour: blue – vacuole, light-blue – cytosol, green – chloroplast, orange – mitochondria, light-orange – peroxisome. The main enzymes involved in this process are shown in green. Molecules with ^{13}C in red type indicate metabolites labelled in the isotope labelling kinetic experiment. Question marks (?) indicate transporters for which the presence or function in guard cells is unclear. Enzymes: CA, carbonic anhydrase; Inv, invertase; PEPc, phospho*enol*pyruvate carboxylase; PEPk, phospho*enol*pyruvate carboxykinase; Rbcs, ribulose-1,5-biphosphate carboxylase/oxygenase; SuSy, sucrose synthase. Metabolites: 2OG, 2-oxoglutarate; 3PGA, 3 phosphoglycerate; Ac-CoA, acetyl CoA; Asp, aspartate; cis-Aco, cis aconitate; Cl^-, chloride; CO_2, carbon dioxide; Fru, fructose; Fum, fumarate; Glu, glutamate; Gluc, glucose; Isoc, isocitrate; K^+, potassium; Mal, malate; NO_3^-, nitrate; OAA, oxaloacetate; PEP, phospho*enol* pyruvate; Suc, sucrose; Succ, succinate; Suc-CoA, succinyl Coa; Triose P, triose phosphate; UDP-glu, uridine diphosphate glucose. Transporters: CLC, chloride channel; DC, dicarboxylate carrier; NRT, nitrate transporter; OC, putative oxaloacetate carrier; OGC, oxoglutarate carrier; PC, pyruvate carrier.

(Talbott & Zeiger 1996; Zeiger *et al*. 2002). It is thought to be the main osmolyte in the afternoon period, replacing K^+ accumulated in the morning in order to maintain stomata open (Talbott & Zeiger 1996). Given the complexity and the importance of sucrose metabolism in other cell types, it is perhaps not surprising that sucrose fulfils other roles than that of osmoticum in the control of stomatal movements. However, the lack of data concerning guard cell metabolism have made it difficult to postulate other possible roles of sucrose in guard cell regulation. In this context, sucrose has

also been considered as a possible signal connecting mesophyll photosynthetic activity to guard cell function (Lawson & Blatt 2014; Lawson *et al*. 2014), and the accumulation of sucrose in the apoplast of guard cells is known to induce stomatal opening or closure as a function of the mesophyll photosynthetic activity (Lu *et al*. 1995, 1997; Ritte *et al*. 1999; Kelly *et al*. 2013). Recently, we provided evidence for another role of sucrose within guard cells. Using reverse genetic approaches, we demonstrated that transgenic potato (*Solanum tuberosum* L.) plants expressing an antisense construct targeted against sucrose synthase 3 (SUS3) exhibited decreased stomatal conductance, whereas transgenic potato plants with increased guard cell acid Inv activity increased their stomatal conductance (Antunes *et al*. 2012). These results indicate that sucrose breakdown, and not just its accumulation, is important during stomatal opening.

Here, the decrease in sucrose levels during stomatal opening induced by K^+, which occurred in the absence of changes in starch content and sucrose content in the medium, provides further evidence that sucrose breakdown within guard cells is of clear importance during stomatal opening. Although it is difficult to rule out any release of sugar into the medium, it seems unlikely that release of sucrose could explain the reductions in sucrose content observed (Fig. 1). Furthermore, the increase in sucrose content observed under sucrose treatment, probably a combined effect of both sucrose influx and guard cell photosynthesis, was accompanied by an increase in fructose and glucose without changes in starch content, indicating that the increase in fructose and glucose comes from sucrose, as opposed to starch breakdown.

Collectively, these results highlight the importance of sucrose as a substrate for guard cell regulation in addition to its role as an active osmoticum. Given that SuSy activity was several fold higher in guard cells than in leaves and the opposite was observed for Inv, coupled with higher SuSy activity than alkaline Inv activity in guard cells, we suggest that sucrose breakdown in the cytosol of guard cells *in vivo* is predominantly catalysed by SuSy rather than by Inv. It is important to highlight that guard cells represent only a small proportion of the mass of epidermal fragments as most of the mass is composed of dead epidermal and pavement cells. This means that enzyme activity will be underestimated in guard cells when determined on a fresh weight basis. However, even with this possible underestimation, SuSy activity was ~40-fold higher in guard cell-enriched epidermal fragments than in leaves on fresh weight basis. In addition higher SuSy activity was also found in epidermal fragments on a protein basis, indicating that SuSy activity is likely to have a great influence on stomatal aperture. Indeed, these data agree with measurements of expression of SuSy isoforms in *Arabidopsis* where SUS3 has been shown to be highly expressed in guard cells in comparison with whole leaves (Bieniawska *et al*. 2007; Bates *et al*. 2012) as well as with the impact that genetic manipulation of SUS3 isoform has in stomatal conductance (Antunes *et al*. 2012). However, these results do not diminish the importance of Inv for guard cell regulation given the higher acid Inv activity in guard cells compared with SuSy activity. This higher acid Inv activity is related to the cleavage of sucrose in the vacuole and not in the apoplast space, given that the Inv activity measured is related to soluble proteins (Roitsch & González 2004; Wang *et al*. 2010). Thus, it seems likely that sucrose breakdown in guard cells would occur predominantly by SuSy in the cytosol and Inv in the vacuole. However, further experiments are needed to better understand how Inv and SuSy regulate the sucrose levels in both cytosol and vacuole during stomatal opening.

The sucrose breakdown hypothesis has already been proposed to occur in order to provide carbon skeletons for organic acid production (Dittrich & Raschke 1977), which in turn can be stored in the vacuole to act as counter ions of K^+ (Hedrich & Marten 1993) or can act as a signal for the activation of the vacuole Cl^- transporter *aluminium-activated malate transporter 9* (ALMT9) (De Angeli *et al*. 2013) (Fig. 9). Given the high respiratory rate of guard cells (Vani & Raghavendra 1994), sucrose may also be metabolized to provide substrate for respiration. We further discuss the possible metabolic fate of carbon following sucrose breakdown below.

Connecting sucrose breakdown and organic acid production during light-induced stomatal opening

The increase in ^{13}C enrichment in malate during the light- and K^+-induced stomatal opening that we observed is what would be anticipated based on the literature (Hedrich & Marten 1993; Talbott & Zeiger 1993), suggesting that the methodology used here is appropriate. Malate is the main organic acid involved in stomatal movements, acting as counter ion of K^+ and substrate for respiration during stomatal opening (Hedrich & Marten 1993) as well as signalling molecule in the guard cell apoplast communicating mesophyll cells and guard cells during stomatal closure induced by CO_2 (Lee *et al*. 2008; Negi *et al*. 2008; Kim *et al*. 2010). Fumarate that exhibits some similarities to malate including chemical structure, pattern of accumulation and degradation throughout the day and ability to induce stomatal closure in a dose-dependent manner (Nunes-Nesi *et al*. 2007; Araújo *et al*. 2011b,c) may have a similar role to malate in guard cells. However, given that malate is present in the guard cell apoplast at higher concentrations (Araújo *et al*. 2011b), it would seem likely that it exerts greater influence on stomatal opening than fumarate does *in vivo* (Araújo *et al*. 2011a,c).

The increase in ^{13}C enrichment observed in malate, fumarate, succinate and glutamate as well as the increase observed in the abundance of these metabolites during light-induced stomatal opening provides evidence for the operation of the TCA cycle during this process. The decrease in levels of sucrose observed under K^+ treatment coupled with increases in abundance and ^{13}C enrichment of TCA cycle intermediates suggests that sucrose breakdown may occur to provide carbon for glycolysis and mitochondrial metabolism. The lower ^{13}C enrichment observed in malate and fumarate under sucrose treatment compared with K^+ treatment may

arise from the incorporation of ^{12}C atoms derived from breakdown of unlabelled sucrose taken up from the medium. These results suggest that sucrose breakdown may contribute towards meeting the carbon requirements for the operation of TCA cycle. Alternatively, the higher ^{13}C enrichment in malate and fumarate under K^+ treatment may be the result of increased demand for ATP or carbon skeletons and hence increased flux towards production of these TCA cycle intermediates. Given that we did not observed changes in starch content in previous experiment, the source of carbon to the increased flux through the TCA cycle under K^+ treatment seems to likely come from sucrose breakdown.

An increase in abundance and ^{13}C labelling of glutamate was also observed under several treatments. Interestingly, glutamate was not labelled under the control treatment, indicating that the presence of K^+ and sucrose induced carbon flux towards this metabolite. In illuminated leaves, the carbon source for glutamate production comes from 2-oxoglutarate directly from the TCA cycle either using newly formed citrate or via the breakdown of citrate stored during the previous dark period (Fig. 9) (Gauthier *et al*. 2010). Although the role of glutamate in guard cell function is still unknown, the ^{13}C enrichment in glutamate represents additional evidence that the TCA cycle is operating during light-induced stomatal opening. Further feeding experiments using different labelled substrates may help to elucidate whether the carbon from sucrose breakdown is used to fuel organic acid production as well as to demonstrate how the TCA cycle-related metabolites contribute to guard cell function and how the TCA cycle operates in guard cells during the dark-to-light transition.

Can tobacco guard cells produce all the ATP and osmolytes required for stomatal opening?

Starch breakdown in guard cell chloroplasts has been shown to be an important mechanism to increase the level of osmoregulatory molecules, counter ions (mainly malate) and/or substrates for respiration (Shimazaki *et al*. 2007). This mechanism is believed to occur mainly under blue light (Talbott & Zeiger 1993) as blue light-induced stomatal opening was severely impaired in the *Arabidopsis pgm* mutant, which accumulates little to no starch in guard cell chloroplasts (Lascève *et al*. 1997). Guard cell starch content has also been quantitatively related to stomatal aperture in *Vicia faba* (Outlaw & Manchester 1979). However, the relative rates of sugar import/synthesis and consumption could determine whether a net change in the starch content of guard cell actually occurs (Ditrich & Raschke 1977). Therefore, it is not surprising that under certain conditions the starch content of guard cells does not change during stomatal movement (Lawson 2009), as observed here. Interestingly, under control treatment the stomata opened significantly after 8 min and remained open for the rest of the experiment in the absence of changes in starch (Fig. 2). Given that the epidermal fragments were harvested pre-dawn, this fast stomatal opening may be related to the circadian clock of the stomatal opening of plants growing under tropical conditions, in which rapid stomatal opening is observed in early morning (Antunes *et al*. 2012; Rodríguez-López *et al*. 2013). These results suggest that guard cells are either fixing the carbon needed to produce the osmoticum required to open the stomatal pore via photosynthesis or alternatively have stored this carbon in another form, most likely in the vacuole, during the previous dark period.

Given that we worked with guard cell-enriched epidermal fragments that are not subject to the mesophyll effect on guard cell movements, the fact that the stomatal pore opens in the light without the addition of sucrose and K^+ suggests that guard cells are producing all the ATP required for stomatal opening in response to light. It has been previously suggested that the energetic demand for stomatal opening can be efficiently met by guard cells (Humble & Hsiao 1970; Inoue *et al*. 1985; Tominaga *et al*. 2001; Zeiger *et al*. 2002). Furthermore, although evidence demonstrating that stomatal responses to light are dependent on the photosynthetic rates of mesophyll cells (Shimazaki *et al*. 2007; Doi & Shimazaki 2008; Mott 2009) and that the level of TCA cycle intermediates from mesophyll cells can influence stomatal conductance (Nunes-Nesi *et al*. 2007; Araújo *et al*. 2011b), there are other examples where antisense plants for cytochrome b_6f complex (Baroli *et al*. 2008), SBPase (Lawson *et al*. 2008) and Rubisco (von Caemmerer *et al*. 2004; Baroli *et al*. 2008) showed no changes in stomatal conductance. Apparently, guard cells are able to produce both ATP and osmolytes necessary for stomatal opening, at least under the conditions used here, which can partially explain the lack of changes observed in starch content.

When taken together, the data presented here strongly indicate a simultaneous CO_2 fixation by Rubisco and PEPcase. It should be mentioned, however, that they do not enable us to distinguish the relative importance of each pathway for guard cell function. Furthermore, the results showed here suggest that during light-induced stomatal opening sucrose breakdown can be an important mechanism to provide carbon skeletons for the production of metabolites of, or associated with, the TCA cycle. Furthermore, sophisticated feeding experiments coupled with analysis of guard cell photosynthesis and respiratory measurements may aid in unravelling further complexities of guard cell metabolism.

ACKNOWLEDGMENTS

This research was supported by the CNPq (National Council for Technological and Scientific Development, Brazil) and FAPEMIG (Foundation for Research Assistance of the Minas Gerais State, Brazil). D.M.D. was the recipient of a scholarship from the FAPEMIG and T.C.R.W. acknowledges the support of CAPES (CAPES-PVE grant). Post-doctoral and research fellowships granted by CNPq to D.M.D. and W.L.A., respectively, are also gratefully acknowledged.

CONFLICTS OF INTEREST

The authors declare that the research was conducted in the absence of any commercial or financial relationships that could be construed as a potential conflict of interest.

REFERENCES

Andrés Z., Pérez-Hormaeche J., Leidi E.O., Schlücking K., Steinhorst L., McLachlan D.H., . . . Pardo J.M. (2014) Control of vacuolar dynamics and regulation of stomatal aperture by tonoplast potassium uptake. *Proceedings of the National Academy of Sciences of the United States of America* **111,** 1806–1814.

Antunes W.C., Provart N.J., Williams T.C.R. & Loureiro M.E. (2012) Changes in stomatal function and water use efficiency in potato plants with altered sucrolytic activity. *Plant, Cell & Environment* **35,** 747–759.

Araújo W.L., Fernie A.R. & Nunes-Nesi A. (2011a) Control of stomatal aperture: a renaissance of the old guard. *Plant Signaling and Behavior* **6,** 1305–1311.

Araújo W.L., Nunes-Nesi A., Osorio S., Usadel B., Fuentes D., Nagy R., . . . Fernie A.R. (2011b) Antisense inhibition of the iron–sulphur subunit of succinate dehydrogenase enhances photosynthesis and growth in tomato via an organic acid-mediated effect on stomatal aperture. *The Plant Cell* **23,** 600–627.

Araújo W.L., Nunes-Nesi A. & Fernie A.R. (2011c) Fumarate: multiple functions of a simple metabolite. *Phytochemistry* **72,** 838–843.

Baroli I., Price G.D., Badger M.R. & von Caemmerer S. (2008) The contribution of photosynthesis to the red light response of stomatal conductance. *Plant Physiology* **146,** 737–747.

Bates G.W., Rosenthal D.M., Sun J., Chattopadhyay M., Peffer E., Yang J., . . . Jones A.M. (2012) A comparative study of the *Arabidopsis thaliana* guard-cell transcriptome and its modulation by sucrose. *PLoS ONE* **7,** e49641.

Bieniawska Z., Barratt D.H.P., Garlick A.P., Thole V., Kruger N.J., Martin C., . . . Smith A.M. (2007) Analysis of the sucrose synthase gene family in *Arabidopsis*. *The Plant Journal* **49,** 810–828.

Bradford M.M. (1976) A rapid and sensitive method for the quantitation of microgram quantities of protein utilizing the principle of protein-dye binding. *Analytical Biochemistry* **72,** 248–254.

Brown P.H. & Outlaw W.H. Jr. (1982) Effect of fusicoccin on dark $^{14}CO2$ fixation by *Vicia faba* guard cell protoplasts. *Plant Physiology* **70,** 1700–1703.

von Caemmerer S., Lawson T., Oxborough K., Baker N.R., Andrews T.J. & Raines C.A. (2004) Stomatal conductance does not correlate with photosynthetic capacity in transgenic tobacco with reduced amounts of RubisCO. *Journal of Experimental Botany* **55,** 1157–1166.

Chen C., Xiao Y.G., Li X. & Ni M. (2012) Light-regulated stomatal aperture in *Arabidopsis*. *Molecular Plant* **5,** 566–572.

Cockburn W. (1983) Stomatal mechanism as the basis of the evolution of CAM and C4 photosynthesis. *Plant, Cell & Environment* **6,** 275–279.

Colón A.J.M., Morgan J.A., Dudareva N. & Rhodes D. (2009) Application of dynamic flux analysis in plant metabolic networks. In *Plant Metabolic Networks* (ed. J. Schwender), pp. 285–305. Springer, New York.

De Angeli A., Zhang J., Meyer S. & Martinoia E. (2013) AtALMT9 is a malate-activated vacuolar chloride channel required for stomatal opening in *Arabidopsis*. *Nature Communications* **4,** 1–10.

Dittrich P. & Raschke K. (1977) Malate metabolism in isolated epidermis of *Commelina communis* L. *Planta* **134,** 77–81.

Doi M. & Shimazaki K.I. (2008) The stomata of the fern *Adiantum capillus-veneris* do not respond to CO_2 in dark and open by photosynthesis in guard cells. *Plant Physiology* **147,** 922–930.

Fernie A.R. & Morgan J.A. (2013) Analysis of metabolic flux using dynamic labelling and metabolic modelling. *Plant, Cell & Environment* **36,** 1738–1750.

Fernie A.R., Geigenberger P. & Stitt M. (2005) Flux an important, but neglected, component of functional genomics. *Current Opinion in Plant Biology* **8,** 174–182.

Fischer R.A. (1971) Role of potassium in stomatal opening in the leaf of *Vicia faba*. *Plant Physiology* **47,** 555–558.

Fischer R.A. & Hsiao T.C. (1968) Stomatal opening in isolated epidermal strips of *Vicia faba*. II. Responses to KCl concentration and the role of potassium absorption. *Plant Physiology* **43,** 1953–1958.

Gauthier P.P., Bligny R., Gout E., Mahé A., Nogués S., Hodges M. & Tcherkez G.G. (2010) In folio isotopic tracing demonstrates that nitrogen assimilation into glutamate is mostly independent from current CO_2 assimilation in illuminated leaves of *Brassica napus*. *The New Phytologist* **185,** 988–999.

Gautier H., Vavasseur A., Gans P. & Lasceve G. (1991) Relationship between respiration and photosynthesis in guard cell and mesophyll cell protoplasts of *Commelina communis* L. *Plant Physiology* **95,** 636–641.

Gibon Y., Blaesing O.E., Hannemann J., Carillo P., Höhne M., Hendriks J.H.M. & Stitt M. (2004) A robot-based platform to measure multiple enzyme activities in *Arabidopsis* using a set of cycling assays: comparison of changes of enzyme activities and transcript levels during diurnal cycles and in prolonged darkness. *The Plant Cell* **16,** 3304–3325.

Gotow K., Taylor S. & Zeiger E. (1988) Photosynthetic carbon fixation in guard cell protoplasts of *Vicia faba*: evidence from radiolabel experiments. *Plant Physiology* **86,** 700–705.

Guo F.Q., Young J. & Crawford N.M. (2003) The nitrate transporter AtNRT1.1 (CHL1) functions in stomatal opening and contributes to drought susceptibility in *Arabidopsis*. *The Plant Cell* **15,** 107–117.

Hedrich R. & Marten I. (1993) Malate-induced feedback regulation of plasma membrane anion channels could provide a CO_2 sensor to guard cells. *The EMBO Journal* **12,** 897–901.

Heise R., Arrivault S., Szecowka M., Tohge T., Nunes-Nesi A., Stitt M. & Fernie A.R. (2014) Flux profiling of photosynthetic carbon metabolism in intact plants. *Nature Protocols* **9,** 1803–1824.

Hetherington A.M. & Woodward F.I. (2003) The role of stomata in sensing and driving environmental change. *Nature* **424,** 901–908.

Huang C.N., Cornejo M.J., Bush D.S. & Jones R.L. (1986) Estimating viability of plant protoplasts using double and single staining. *Protoplasma* **135,** 80–87.

Huege J., Goetze J., Dethloff F., Junker B. & Kopka J. (2014) Quantification of stable isotope label in metabolites via mass spectrometry. *Methods in Molecular Biology* **1056,** 213–223.

Humble G.D. & Hsiao T.C. (1970) Light-dependent influx and efflux of potassium of guard cells during stomatal opening and closing. *Plant Physiology* **46,** 483–487.

Inoue H., Noguchi M. & KuBo K. (1985) Ion-stimulated stomatal opening induced by preillumination in epidermal strips of *Commelina communis*. *Plant Physiology* **79,** 389–393.

Jin X., Wang R., Zhu M., Jeon B.W., Albert R., Chen S. & Assmann S. (2013) Abscisic acid-responsive guard cell metabolomes of *Arabidopsis* wild-type and *gpa1* G-protein mutants. *The Plant Cell* **25,** 4789–4811.

Kang Y., Outlaw W.H. Jr., Anderson P.C. & Fiore G.B. (2007) Guard cell apoplastic sucrose concentration – a link between leaf photosynthesis and stomatal aperture size in apoplastic phloem loader *Vicia faba* L. *Plant, Cell & Environment* **30,** 551–558.

Kelly G., Moshelion M., David-Schwartz R., Halperin O., Wallach R., Attia Z., . . . Granot D. (2013) Hexokinase mediates stomatal closure. *The Plant Journal* **75,** 977–988.

Kim T.H., Böhmer M., Hu H., Nishimura N. & Schroeder J.I. (2010) Guard cell signal transduction network: advances in understanding abscisic acid, CO_2, and Ca^{2+} signaling. *Annual Review of Plant Biology* **61,** 561–591.

Kruse T., Tallman G. & Zeiger E. (1989) Isolation of guard cell protoplasts from mechanically prepared epidermis of *Vicia faba* leaves. *Plant Physiology* **90,** 1382–1386.

Lascève G., Leymarie J. & Vavasseur A. (1997) Alterations in light-induced stomatal opening in a starch-deficient mutant of *Arabidopsis thaliana* L. deficient in chloroplast phosphoglucomutase activity. *Plant, Cell & Environment* **20,** 350–358.

Lawson T. (2009) Guard cell photosynthesis and stomatal function. *The New Phytologist* **181,** 13–34.

Lawson T. & Blatt M.R. (2014) Stomatal size, speed and responsiveness impact on photosynthesis and water use efficiency. *Plant Physiology* **164,** 1556–1570.

Lawson T., Lefebvre S., Baker N.R., Morison J.I.L. & Raines C. (2008) Reductions in mesophyll and guard cell photosynthesis impact on the control of stomatal responses to light and CO_2. *Journal of Experimental Botany* **59,** 3609–3619.

Lawson T., Simkin A.J., Kelly G. & Granot D. (2014) Mesophyll photosynthesis and guard cell metabolism impacts on stomatal behaviour. *The New Phytologist* **203,** 1064–1081.

Lee M., Choi Y., Burla B., Kim Y.Y., Jeon B., Maeshima M., . . . Lee Y. (2008) The ABC transporter AtABCB14 is a malate importer and modulates stomatal response to CO_2. *Nature Cell Biology* **10,** 1217–1223.

Leonhardt N., Kwak J.M., Robert N., Waner D., Leonhardt G. & Schroeder J.I. (2004) Microarray expression analyses of *Arabidopsis* guard cells and isolation of a recessive abscisic acid hypersensitive protein phosphatase 2C mutant. *The Plant Cell* **16,** 596–615.

Lisec J., Schauer N., Kopka J., Willmitzer L. & Fernie A.R. (2006) Gas chromatography mass spectrometry-based metabolite profiling in plants. *Nature Protocols* **1,** 387–396.

Lu P., Zhang S.Q., Outlaw W.H. Jr. & Riddle K.A. (1995) Sucrose: a solute that accumulates in the guard-cell-apoplast and guard cell symplast of open stomata. *FEBS Letters* **326,** 180–184.

Lu P., Outlaw W.H. Jr., Smith B.G. & Freed G.A. (1997) A new mechanism for the regulation of stomatal aperture size in intact leaves – accumulation of mesophyll-derived sucrose in the guard-cell wall of *Vicia faba*. *Plant Physiology* **114,** 109–118.

MacRobbie E.A.C. (1981) Ion fluxes in isolated guard cells of *Commelina comunis* L. *Journal Experimental of Botany* **32,** 545–562.

MacRobbie E.A.C. (2006) Control of volume and turgor in stomatal guard cells. *The Journal of Membrane Biology* **210,** 131–142.

Medeiros D.B., Daloso D.M., Fernie A.R., Nikoloski Z. & Araújo W.L. (2015) Utilizing systems biology to unravel stomatal function and the hierarchies underpinning its control. *Plant, Cell & Environment* doi: 10.1111/pce.12517.

Mott K.A. (2009) Opinion: stomatal responses to light and CO_2 depend on the mesophyll. *Plant, Cell & Environment* **32,** 1479–1486.

Murashige T. & Skoog F. (1962) A revised medium for rapid growth and bioassays with tobacco tissue cultures. *Physiologia Plantarum* **15,** 473–497.

Negi J., Matsuda O., Nagasawa T., Oba Y., Takahashi H., Kawai-Yamada M., . . . Iba K. (2008) CO_2 regulation SLAC1 and its homologues are essential for anion homeostasis in plant cells. *Nature* **452,** 483–488.

Nunes-Nesi A., Carrari F., Gibon Y., Sulpice R., Lytovchenko A., Fisahn J. & Fernie A.R. (2007) Deficiency of mitochondrial fumarase activity in tomato plants impairs photosynthesis via an effect on stomatal function. *The Plant Journal* **50,** 1093–1106.

Outlaw W.H. Jr. (1989) Critical examination of the quantitative evidence for and against photosynthetic CO_2 fixation in guard cells. *Physiologia Plantarum* **77,** 275–281.

Outlaw W.H. Jr. (1995) Sucrose and stomata: a full circle. In *Carbon Partitioning and Source–Sink Interactions in Plants* (eds M.A. Madore & W.J. Lucus), pp. 56–67. American Society of Plant Physiologists, Rockville, MD, USA.

Outlaw W.H. Jr. (2003) Integration of cellular and physiological functions of guard cells. *Critical Reviews in Plant Sciences* **22,** 503–529.

Outlaw W.H. Jr. & Kennedy J. (1978) Enzymic and substrate basis for the anaplerotic step in guard cells. *Plant Physiology* **62,** 648–652.

Outlaw W.H. Jr. & Manchester J. (1979) Guard cell starch concentration quantitatively related to stomatal aperture. *Plant Physiology* **64,** 79–82.

Outlaw W.H. Jr., Manchester J., Di Camelli C.A., Randall D.D., Rapp B. & Veither G.M. (1979) Photosynthetic carbon reduction pathway is absent in chloroplasts of *Vicia faba* guard cells. *Proceedings of the National Academy of Sciences of the United States of America* **76,** 6371–6375.

Parvathi K. & Raghavendra A.S. (1997) Both RubisCO and phosphoenolpyruvate carboxylase are beneficial for stomatal function in epidermal strips of *Commelina benghalensis*. *Plant Science* **124,** 153–157.

Ratcliffe R.G. & Shachar-Hill Y. (2006) Measuring multiple fluxes through plant metabolic networks. *The Plant Journal* **45,** 490–511.

Ritte G., Rosenfeld J., Rohrig K. & Raschke K. (1999) Rates of sugar uptake by guard cell protoplasts of *Pisum sativum* L. Related to the solute requirement for stomatal opening. *Plant Physiology* **121,** 647–656.

Rodríguez-López N.F., Cavatte P.C., Silva P.E.M., Martins S.C.V., Morais L.E., Medina E.F. & DaMatta F.M. (2013) Physiological and biochemical abilities of robusta coffee leaves for acclimation to cope with temporal changes in light availability. *Physiologia Plantarum* **149,** 45–55.

Roessner-Tunali U., Luedemann A., Brust D., Fiehn O., Linke T., Willmitzer L. & Fernie A.R. (2001) Metabolic profiling allows comprehensive phenotyping of genetically or environmentally modified plant systems. *The Plant Cell* **13,** 11–29.

Roessner-Tunali U., Liu J., Leisse A., Balbo I., Perez-Melis A., Willmitzer L. & Fernie A.R. (2004) Kinetics of labeling of organic and amino acids in potato tubers by gas chromatography-mass spectrometry following incubation in ^{13}C labeled isotopes. *The Plant Journal* **39,** 668–679.

Roitsch T. & González M.C. (2004) Function and regulation of plant invertases: sweet sensations. *Trends in Plant Science* **9,** 606–613.

Sayre J.D. (1923) Physiology of stomata of *Rutiilex Patlitioh*. *Science* **57,** 205–206.

Sayre J.D. (1926) Physiology of stomata of *Rumex patientia*. *The Ohio Journal of Science* **26,** 233–266.

Shimazaki K.I., Doi M., Assmann S.M. & Kinoshita T. (2007) Light regulation of stomatal movements. *Annual Review of Plant Biology* **58,** 219–247.

Stitt M., Lilley R.M., Gerhardt R. & Heldt H.W. (1989) Metabolite levels in specific cells and subcellular compartments of plant leaves. *Methods in Enzymology* **174,** 518–552.

Studart-Guimarães C., Fait A., Nunes-Nesi A., Carrari F., Usadel B. & Fernie A.R. (2007) Reduced expression of succinyl-coenzyme a ligase can be compensated for by up-regulation of the γ-aminobutyrate shunt in illuminated tomato leaves. *Plant Physiology* **145,** 626–639.

Suetsugu N., Takami T., Ebisu Y., Watanabe H., Iiboshi C., Doi M. & Shimazaki K.I. (2014) Guard cell chloroplasts are essential for blue light-dependent stomatal opening in *Arabidopsis*. *PLoS ONE* **9,** 108374.

Szecowka M., Heise R., Tohge T., Nunes-Nesi A., Vosloh D., Huege J. & Arrivault S. (2013) Metabolic fluxes in an illuminated *Arabidopsis* rosette. *The Plant Cell* **25,** 694–714.

Talbott L.D. & Zeiger E. (1993) Sugar and organic acid accumulation in guard cells of *Vicia faba* in response to red and blue light. *Plant Physiology* **102,** 1163–1169.

Talbott L.D. & Zeiger E. (1996) Central roles for potassium and sucrose in guard-cell osmoregulation. *Plant Physiology* **111,** 1051–1057.

Talbott L.D. & Zeiger E. (1998) The role of sucrose in guard cell osmoregulation. *Journal of Experimental Botany* **49,** 329–337.

Tallman G. & Zeiger E. (1988) Light quality and osmoregulation in *Vicia* guard cells. *Plant Physiology* **88,** 887–895.

Tarczynski M.C., Outlaw W.H. Jr., Arold N., Neuhoff V. & Hampp R. (1989) Electrophoretic assay for ribulose 1, 5-bisphosphate carboxylase/oxygenase in guard cells and other leaf cells of *Vicia faba* L. *Plant Physiology* **89,** 1088–1093.

Tominaga M., Kinoshita T. & Shimazaki K. (2001) Guard cell chloroplasts provide ATP for H^+ pumping in the plasma membrane and stomatal opening. *Plant and Cell Physiology* **42,** 795–802.

Trethewey R.N., Riesmeier J.W., Willmitzer L., Stitt M. & Geigenberger P. (1999) Tuber-specific expression of a yeast invertase and a bacterial glucokinase in potato leads to an activation of sucrose phosphate synthase and the creation of a sucrose futile cycle. *Planta* **208,** 227–238.

Vani T. & Raghavendra A.S. (1994) High mitochondrial activity but incomplete engagement of the cyanide-resistant alternative pathway in guard cell protoplasts of pea. *Plant Physiology* **105,** 1263–1268.

Vavasseur A. & Raghavendra A.S. (2005) Guard cell metabolism and CO2 sensing. *The New Phytologist* **165,** 665–682.

Wang L., Li X.R., Lian H., Ni D.A., He Y.K., Chen X.Y. & Ruan Y.L. (2010) Evidence that high activity of vacuolar invertase is required for cotton fiber and *Arabidopsis* root elongation through osmotic dependent and independent pathways, respectively. *Plant Physiology* **154,** 744–756.

Wang S.W., Li Y., Zhang X.L., Yang H.Q., Han X.F., Liu Z.H. & Chen Y.L. (2014) Lacking chloroplasts in guard cells of *crumpled leaf* attenuates stomatal opening: both guard cell chloroplasts and mesophyll contribute to guard cell ATP levels. *Plant, Cell & Environment* **37,** 2201–2210.

Willmer C.M. & Dittrich P. (1974) Carbon dioxide fixation by epidermal and mesophyll tissues of *Tulipa* and *Commelina*. *Planta* **177,** 123–132.

Yang H.M., Zhang J.H. & Zhang X.Y. (2005) Regulation mechanisms of stomatal oscillation. *Acta Botanica Sinica* **47,** 1159–1172.

Yang Y., Costa A., Leonhardt A., Siegel R.S. & Schroeder J.I. (2008) Isolation of a strong *Arabidopsis* guard cell promoter and its potential as a research tool. *Plant Methods* **4,** 6.

Zeiger E. (1983) The biology of stomatal guard cells. *Annual Review of Plant Physiology* **34,** 441–475.

Zeiger E., Talbott L.D., Frechilla S., Srivastava A. & Zhu J. (2002) The guard cell chloroplast: a perspective for the twenty-first century. *The New Phytologist* **153,** 415–424.

Zhao Z., Zhang W., Stanley B.A. & Assmann S.M. (2008) Functional proteomics of *Arabidopsis thaliana* guard cells uncovers new stomatal signaling pathways. *The Plant Cell* **20,** 3210–3226.

Zhu M., Dai S., McClung S., Yan X. & Chen S. (2009) Functional differentiation of *Brassica napus* guard cells and mesophyll cells revealed by comparative proteomics. *Molecular and Cellular Proteomics* **8,** 752–766.

Zhu M., Simons B., Zhu N., Oppenheimer D.G. & Chen S. (2010) Analysis of abscisic acid responsive proteins in *Brassica napus* guard cells by multiplexed isobaric tagging. *Journal of Proteomics* **73,** 790–805.

Zhu M., Zhu N., Song W.Y., Harmon A.C., Assmann S.M. & Chen S. (2014) Thiol-based redox proteins in abscisic acid and methyl jasmonate signaling in *Brassica napus* guard cells. *The Plant Journal* **78,** 491–515.

Zrenner R., Salanoubat M., Willmitzer L. & Sonnewald U. (1995) Evidence for the crucial role of sucrose synthase for sink strength using transgenic potato plants (*Solanum tuberosum* L.). *The Plant Journal* **7,** 97–107.

Received 28 January 2015; received in revised form 7 April 2015; accepted for publication 9 April 2015

SUPPORTING INFORMATION

Additional Supporting Information may be found in the online version of this article at the publisher's web-site:

Figure S1. Material used in the light-induced stomatal opening experiments. (a) Pictures (top) showing the distribution of Petri dishes with guard cell-enriched epidermal fragments between two water layers to avoid heat excess. Thermal imaging (below) confirming the lack of heating of samples. (b) Pictures of stomata from light-induced stomatal opening experiments using guard cell-enriched epidermal fragments in different treatment solutions. The guard cell-enriched epidermal fragments were incubated in solutions containing MES/NaOH (5 mM) pH 6.5 + $CaCl_2$ 50 μM + mannitol 20 mM; + KCl 5 mM); KCl + sucrose (MES/NaOH 5 mM pH 6.5 + $CaCl_2$ 50 μM + KCl 5 mM + sucrose 20 mM). Black bar = 5 μm. (c) Stomatal aperture measurements in guard cell-enriched epidermal fragments incubated in the solutions described earlier maintained under dark or light conditions ($n = 4 \pm$ SE). (d) Fluorescence photomicrography of guard cell-enriched epidermal fragments highlighting the viability of guard cells, and absence of intact other pavement epidermal cells. Cells were stained with both fluorescein diacetate (FDA, green – living cells) and propidium iodide (PI, red – dead cells).

Figure S2. The relationship between stomatal aperture and level of sugars in guard cells. A linear regression was performed as the increase in stomatal aperture and the decrease in sucrose (a), glucose (b), fructose (c) and the sum of these sugars (d) observed in Fig. 1. The significance of the regression is shown in the graph by *P*-values.

Figure S3. Metabolite contents (nmol μL^{-1}) in the medium used during light- and potassium-induced stomatal opening experiment shown in Fig. 1. Guard cell-enriched epidermal fragments were incubated in the light for 0, 40, 80 and 120 min under MES buffer solution (MES + $CaCl_2$ + mannitol) or K^+ solution (MES + $CaCl_2$ + KCl). An aliquot of the medium was collected at each time point in order to determine the level of sugars. No differences in the level of sugars were detected over time ($n = 4 \pm$ SE).

Figure S4. Metabolite levels (relative to ribitol g^{-1} of fresh weight – FW) in guard cell-enriched epidermal fragment of *Nicotiana tabacum*. Control, MES + $CaCl_2$ + mannitol; K^+, MES + $CaCl_2$ + KCl; K^+ + S, MES + $CaCl_2$ + KCl + sucrose; sucrose, MES + $CaCl_2$ + sucrose. Data presented are mean ± SE ($n = 4$). The significance of the influence of both time and treatment in the level of each metabolite was analysed by ANOVA and Dunnett's test and is shown in Supporting Information Table S1. Asterisks indicate values significantly different from the control treatment in the same time point by Student's *t*-test ($P < 0.05$).

Table S1. ANOVA of metabolic profile.

Dataset S1. Metabolite reporting guidelines (checklist table).